University of Cincinnati

Date: 2/26/2020

I, Yunzheng He, hereby submit this original work as part of the requirements for the degree of Master of Science in Aerospace Engineering.

It is entitled:

Modeling and Simulation of Tensegrity Structure based on SimMechanics

Student's name: **Yunzheng He**

This work and its defense approved by:

Committee chair: Kelly Cohen, Ph.D.

Committee member: Anoop Sathyan, PhD

Committee member: George T. Black, M.S.

Committee member: Wei Wei, Ph.D.

UNIVERSITY OF Cincinnati

36583

Modeling and Simulation of Tensegrity Structure based on SimMechanics

A Thesis Submitted to the
Graduate School of the University of Cincinnati
in Partial Fulfillment of the
Requirements for the Degree of

Master of Science

in the Department of Aerospace Engineering
of the College of Engineering & Applied Science

By
Yunzheng He

B.S. Beijing Forestry University

February 20, 2020

Committee Chair: Kelly Cohen, PhD.

ABSTRACT

The research and development process of tensegrity structures has thus far been to analyze the mathematical model then utilize physical models to prove new theories. This process is time-consuming and costly. It is in researchers' as well as the private sectors' best interests to shorten this process as much as possible without resulting in false conclusions. This thesis proves that we can do just that by adopting a novel method of performing tensegrity vibration and control simulations. This method uses Simulink in conjunction with a specialized module in MATLAB, SimMechanics.

To study this new method, we built a complete model of a Class-Two, Five-Layer tensegrity tower in SimMechanics. Actuators and sensors are attached to the structure to carry out simulations. The Five-Layer tower was then modified into a Three_Layer one to carry out forced vibration experiments using base excitation of the structure through chirp signals were performed and the dynamic responses were recorded and compared to previous experimental results. Next, A One-Layer tensegrity robot model was built to conduct dynamic and control simulations. PID controller was also introduced to the model, and step response simulation results were plotted and analyzed. The experimental results indicate that a computational modeling and research approach is an effective and accurate modeling approach for tensegrity structures.

ACKNOWLEDGEMENTS

I would like to thank Dr. Kelly Cohen from the University of Cincinnati for all his guidance, support, and assistance. He introduced me to this exciting field of tensegrity structures. I would also like to thank Wei Wei for his help and discussions during my research. Finally, I want to express my deepest gratitude my family and my girlfriend Elyse for all their encouragement and support during my long course of pursuing the master's degree in aerospace engineering.

TABLE OF CONTENTS

LIST OF FIGURES

LIST OF TABLES

CHAPTER 1: INTRODUCTION

Coined by Buckminster Fuller as a contraction for the two words tension and integrity, the definition of tensegrity configuration, as presented by Robert E. Skelton in the book, Tensegrity System, follows:

In the absence of external forces, let a set of rigid bodies in a specific configuration have torqueless connections (e.g. via frictionless ball-joints). Then this configuration forms a tensegrity configuration if the given configuration can be stabilized by some set of internal tensile members, i.e. connected between the rigid bodies. The configuration is not a tensegrity configuration if no tensile members are required or no set of tensile members exist to stabilize the configuration [1].

By definition, there must exist stabilizing connectivity for each tensegrity system, although the actual implementation may not be stable. For this paper, we will only be focusing on those stable configurations.

We would also like to further distinguish between various types of tensegrity systems with the following definition: A tensegrity configuration is called a class 1 tensegrity system if there are no contacts between its rigid bodies, it's called a class k tensegrity system if there are as many as k rigid bodies in contact.

Figure 1 illustrates the first-ever three-dimensional tensegrity structure built by Snelson in 1948. It is a class 1 stable structure since there is no contact between the upper and lower "X" pieces. It is also worthwhile to point out that although one might find the six of the outside tendons are "fake" in the sense that the structure stability will not be affected by removing them. They are not fake in this structure since they counter the inward pull of the tendons that support the "X" form at the crossing.

Figure 1: Snelson's X-module

Source: [2]

In this chapter, we explain the motivation behind our research. Furthermore, we describe our objective and state the problem present.

1.1 Motivation

Lightweight yet strong structure has always been an important topic in product design in the aviation industry. As global trends to CO_2 reduction and resource efficiency increases, new demands for such structures arise. Aside from aviation, tensegrity structures also have great potential in architectural engineering once it can be mathematically proven that they can be designed to take tension, compression or bending. Tensegrity systems are composed of struts and strings, each component is either in compression or in tension. Cables and strings may be used for the components in tension, thus greatly reduce system mass weight and moment of inertia. As such, compared to traditional mechanism, tensegrity structures are more mass efficient, deployable, scalable and redundant [3]. This is especially attractive to space application projects. As Kenneth Snelson puts in his paper "A space station framed according to such a system could be attractive to rocketeers who must count every gram they boost into orbit" [4]. Current research of tensegrity structures can be categorized into two major areas: form-finding and shape control. Both involve a lot of work to be done in either mathematical modeling or hardware set-ups. This research adopts a method using the latest modeling software SimMechanics to achieve tensegrity simulations. Studies have done in the past usually involves the construction of an actual tensegrity structure which is labor and financially costly. Another problem with the physical model is it becomes troublesome to modify the physical configuration once the mechanism has been constructed.

1.2 Thesis Objective

The main aim of this thesis is to prove that it is possible to study the static and dynamic nature of the tensegrity structures with a computational modeling tool, i.e. SimMechanics. With this premise, a class-1 tensegrity tower is modeled using SimMechanics, static simulations have been carried out, next we explored tensegrity robotic dynamic and control experiments. Furthermore, experimental results are analyzed and compared to those obtained from the physical models.

1.3 Thesis Overview

The problem will be examined for a tensegrity structure as pictured in Figure 2, further simplified by assumptions of symmetry and uniformity. The structure is taken as a right regular prism, in which the end faces are equilateral triangles, perpendicular to the axis joining their centroids. The tensegrity position, shown to be globally unique, then is known to require a $\pi/6$ relative rotation between the triangles. A basic tensegrity unit that was adopted for analysis is called a 3-Strut tensegrity prism (t-prism), consisting of 3 compressive struts and 9 tensile strings. It is the simplest and, therefore, one of the most typical members of the tensegrity family.

The three bars are assumed to be rigid, and the three cables comprising the edges of the end face inextensible, while the three diagonal cables are linearly elastic with equal moduli. Any applied force will be required to be symmetric about the axis of the prism. The result of these simplifications is that the triangular faces remain parallel and centered on the z-axis so that all nodal displacements can be described by the angle of relative rotation or by the concomitant vertical displacement. The infinitesimal flexure of the system is an infinitesimal rotation of the upper triangle about its axis.

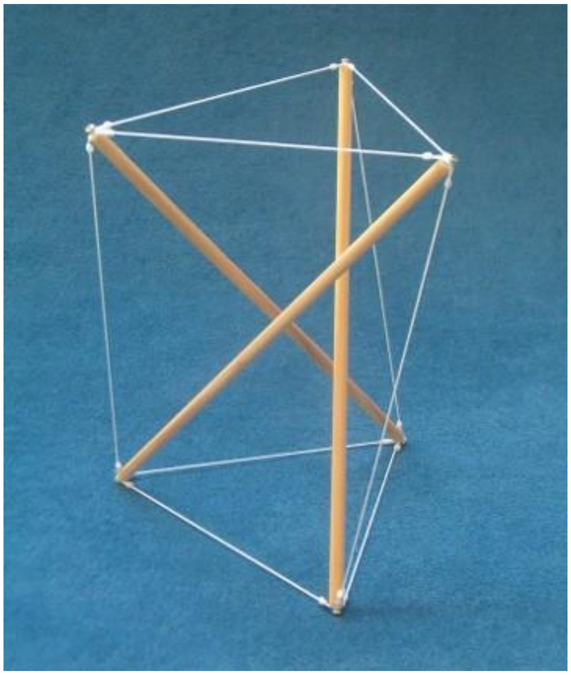

Figure 2: 3-Strut Tensegrity Prism

Source: [5]

In this thesis, we first introduce the concept of tensegrity structures and their constructions. The remainder of the thesis is organized as follows. Chapter 2 provides a literature review in recent tensegrity research development and relevant background knowledge in the SimMechanics modelling environment. Chapter 3 describes methodologies that are used in studying tensegrity structures, both in form-finding and structure analysis. Chapter 4 presents the SimMechanics modeling procedure for a fixed base 3 strut tensegrity structure and carries out forced vibration simulation with SimMechanics model of a tensegrity robot and analyzed simulation results. Chapter 5 makes some concluding remarks, and Chapter 6 provides research outlook in the tensegrity field.

1.4 Thesis Contributions

In this thesis, we present three contributions to the tensegrity modeling and simulation field:

- We present a literature review
- We propose a new modeling and simulation method for tensegrity structure.
- We further extend the modeling application to explore a realization of tensegrity robot.

CHAPTER 2: LITERATURE REVIEW

In this chapter, a review of literature related to the research objective is presented. The literature review was prepared based on the main aim of the thesis which was to prove that it was possible to study both the static and the dynamic nature of the tensegrity structures with computational modeling tools such as SimMechanics.

2.1 Tensegrity Structure Overview

Tensegrity is a type of three-dimensional structure where its string members are under tension, and these members are contiguous while the members under compression are not. In the tensegrity structure, the bars and strings are identified. The strings are the elements that are usually under tension, and the bars are usually under compression. Tensegrity structure has the following properties: they are lightweight, foldable and are also seen to be strong in their making. The strength and the lightness combined make them very strong and deployable as needed in the case of Pulley construction, NiTi wire constructions and more [4].

A special property of tensegrity structures is how the shape of the structure could be changed with very little energy input. The conventional continuous structures when they are changing into a new shape, control energy is required to work against the old equilibrium. However, in the case of a tensegrity structure, shape changes are achieved by changing the equilibrium of the structure, meaning shape controls are inexpensive. This property is in contrast with the classical structures where much energy is needed to change their shapes.

Much of the literature review work hence becomes a contrasting study and not a unique study of features of tensegrities. This work intends to look at the unique features of tensegrities and present their features with respect to more current uses in the construction context. Some of the mechanics of tensegrities would be based on comparing them with classical structures. The concept of self-similar structures is analyzed based on the minimal mass subject, the buckling constraint and the stiffness, strength of structures.

2.2 Characteristics of Tensegrities

The term tensegrity was coined with the words tensional and integrity, referring to the tension and compression components as the integrity of a structure [6]. Researcher Fuller, in [7], explains tensegrity as a system established only when discontinuous compressive components and continuous tensile components integrate into a stable volume in space. Tensegrity, in short, was described by Snelson [8] as something that is discontinuous compression and continuous tension. It was defined as a structural principle, where the system is delineated spatially.

Tensegrity characteristics as understood from different research contexts are presented below. Firstly, tensegrity is considered as more load-bearing compared to any other [6]. Their load-bearing capacity as considered against any other structure of similar weight will be much higher. Secondly, they are very lightweight in comparison that makes them applicable for use even in such situations where a high weight element would be considered dangerous [4].

Thirdly, they are found to have a stronger resistance, which is a much more appreciable strength given that they have better load-bearing capacity even at a much lighter weight. This leads to the benefit of there not needing any other stronger support. This is one of the reasons that they are preferred in construction works. It need not be anchored, so they really don't need any form of surface to lean on, also, they don't depend on elements of weight or gravity. Much of the construction works will need to consider gravity as an important aspect. With tensegrities, the impact of gravity need not be considered to a greater extent. The reason why they can afford not to consider the impact of gravity is that they are stabilized in position by their own compressive and tensile forces. The compressive forces in struts and the tensional forces in prestressed cables help the structure maintain its shape. Analytical solutions of prestressability problem of tensegrity structures have also been studied to derive equilibrium configurations mathematically [9]. The higher the pre-stress that is applied, then the more the structure and its load-bearing capacity. In tensegrity structure, it so happens that the deformation response when a load is placed on it is non-linear. The load increase will result in stiffness of the structure that is similar to how a suspension bridge will operate. Also, an important feature of the structure is how they are modeled with frictionless joints and the self-weight of said structures will normally be neglected.

They are enantiomorphic as well because they can be either right-handed or left-handed as mirror pairs, and this is one reason why the tensegrity modules can be used in such situations as casts, grids, ropes, rings and more [6]. Complex tensegrity structures can be created because of these elements variations.

Tensegrity structures are usually made of such compressive members which are discontinuous and short [6]. An advantage of this is that they do not buckle easily and no torque would be generated in the compressive members. The material used also change the resilience of the structure assembly.

Tensegrity structures are also seen to work in a synergetic manner. What this means, in terms of the tensegrity structures, is that the behavior cannot be predicted as components separately, it has to be predicted by considering the structure as a whole. The synergy is also noticed in the way they behave to stress. For instance, when there is dynamic loading, structures that rely on support might buckle and there is a necessity to be careful. This is not the case with tensegrity structures where the change in load results in a redistribution of the whole weight over the structure. This happens within no time and hence when the structure responds to the weight, it responds as a whole [7]. The ability to respond to as a whole makes it more responsive as a structure.

Finally, there is a term associated with the tensgrity structures called “elastic multiplication”. As shown in [10], elasticity multiplication has a negative correlation to the distance between the two struts of the structure. When two struts are separate by an elongation of the tensile members of the system, then their tensile strength is much less, in contrast with the distance that they are elongated. This property gives tensegrity structures resilience under light loads and makes it stiffen as loading increases.

2.3 Advantages of Tensegrity Structure

Conventional continuous structures have many disadvantages when it comes to strength issues, resistance and even size, and each of these concerns is seen to be advantages when it comes to tensegrity structures.

Firstly, because of its synergetic way of handling loads seem to contribute to missing of critical points of structural weakness. A critical point of weakness is usually a problem when structural loads are added. In the case of tensegrity structures, the lack of the critical load point means there are fewer concerns of breakage. As the whole structure withstands the load, and the load is distributed, the issues of critical points of weakness do not exist.

Secondly, in much of the continuous arrangement in conventional structures, it could so happen that the structures are not uniformly arranged, so there is a torsion effect the system suffers. Some issues of torsion distributed in the whole structure could lead to buckling. In the case of the tensegrity structure, the torsion effect is very much reduced, and even with the inherent issues of space arrangement, and the strut length, the compression is quite uniform because of the load spread and the tensile effects. Therefore, there are no forms of buckling under pressure or loads [11].

While the geometry and the artform, and even the structural appeal in tensegrity is studied in much of the literature context, the understanding of the mechanics of tensegrity and how it can dynamically withstand loading are its core benefits. For instance, form-finding results for symmetric structures seem to indicate much stable integration when working with tensegrity structures [3]. Advanced form-finding structures with respect to tensegrity seem to highlight that tensegrity structures in engineering need much more focus. Tensegrity structures and concept are not that new and have been in existence for around 50 years now but still, it is necessary to study the concept concerning different form-finding contexts in order to understand their dynamics and mechanical benefits.

2.3.1 Tensegrity Has Higher Tension Stability

The nature of a compressive member when it is loaded is to lose its stiffness. This is the nature of the most continuous compressive section. The way stiffness is lost is either in the case of absence of bending moments in the axially loaded struts when the force acts on the mass center, it will increase the diameter of the center cross-section for the compressing member while In the case of the tensile member, the cross-section under load is reduced significantly. In the case of the presence of bending moments, center of mass is offset with the line of force application (http://tensegritywiki.com). The bar becomes much softer because of its bending nature. Stiffness to mass ratio is usually increased in such tensegrity structures by increasing the use of the tensile members.

2.3.2 Load Efficiency of Tensegrity structures

Traditional rectilinear structures are challenged when compared to tensegrity structures. Traditional orthogonal structures have much less strength to withstand different forms of load distribution for a given mass. The material layout will usually have a geometry that is critical for adding strength to the setting, and this is the case for any nanoscale, mega-scale or a biological system. However, traditional layouts only made use of structures that were rectilinear and orthogonal. For example, orthogonal beams and cantilevers were not only used in construction but were also made use of in aircraft wings as well. As shown by Bendsoe and Kikuchi and others [6], in order to achieve specific stiffness objectives, the optimal distribution of mass is neither a solid mass with fixed geometry or orthogonally laid out structure. In the context of tensegrity structures, what happens is that the distribution of mass is only required for laying out in the load path [3]. Only the critical load path is needed. Tensegrity makes use of the longitudinal members that are not orthogonal as well. Strength is hence achieved with a much smaller mass.

2.3.3 Tensegrity Structures are Deployable

Portability of structures is very important. In the case of conventional continuous structures, it would so happen that high strength materials would be minimum displacement capability. For instance, consider piezoelectric materials that are used in industries. Usually, smaller structures that rely on the piezoelectric material will tend to have better displacement capability. Materials of high strength tend to have a very limited displacement capability [12]. In the case of tensegrity structures, their mechanical and dynamic properties make them easy to deploy. Large operational and portability related advantages are hence present because of the use of tensegrity structures. As other examples, consider a portable bridge or a power transmission tower [13]. Now when they are made as tensegrity structures, it would become easier to just port the structures to other places as needed [14]. It could be manufactured in a factory, and then could be transported to the construction site and deployed with as little as transportation structures, cables and winches. Even where the complex mechanical structure cannot be erected on site because of climate conditions or to save costs of erection, the use of these tensegrity structures is helpful [15]. It can save much of the launch costs and eliminate the reassembly requirement on site. Other experts, including Stern [16] have also done research in foldable antenna and some of the results have even been patented.

2.3.4 Tensegrity Structures are Easily Tunable

Researchers argued deployment techniques as contributing much to the value of installing a tensegrity structure versus a continuous conventional structure [17]. It is the deployment technique that is also just as useful when considering how the load can be fine-tuned when using the tensegrity structures [18].

Where the structures allow for much fine-tuning, the mechanical strength of the structure could be improved immensely [19]. In the case of a damaged structure, fine-tuning will allow for better alignment and understanding of structure parameters. Also, with next-generation mechanical structure, it has been identified that fine-tuning would go a long way towards improving the stability of structures as well.

2.3.5 Tensegrity Structures and High Precision Control

Finally, a tensegrity structure allows better precision control as well. Precision modeling is the cornerstone for many structural creations. Tensegrity structures have also shown a high amount of precision control even under dynamic loading. It has been identified that the architecture, the mathematic properties and more of tensile structures are in fact quantum leaps when it comes to adjusting precision from nanoscale levels to the mega-scale levels. It is hence used for such applications where a high degree of precision is required such as that of microsurgery, robotic manipulators, aircraft wings and more.

In addition to facilitating high precision control, tensegrity is also seen to promote a very high standard when it comes to integration of structure. For example, the tensile member can be a load-bearing member, a sensor, and actuator at the same time. The tensegrity designer also faces challenges that what types of controls one could put into such a structure, such as how to implement the electrical energy or how to control the mechanical energy in the structure and more. However, these challenges are small price to pay compared to the entire structural use efficiency that one gets when using tensegrity [3]. For example, consider in an airplane structure, tensegrity could be used as morphing wings to control the aircraft. Similarly, it can also be used to optimize the airfoil.

The element of the tensegrity structure allows for a better transfer of the force. The force is transferred in a very natural manner. The members of the tensegrity are such that they align themselves in order to receive the forces and then transfer them such that they are in alignment with the lines of force. This makes for a very natural transfer after the reception, they perfectly align themselves to retransfer the load in the shortest path possible to preserve their structure from torsion. The force is as transferred in the shortest path possible as well, which means much of the shock and seismic vibration effects in other contexts does not lead to the destruction of the tensegrity material. Since they can absorb shock in a better manner, they are great candidates as actuators and sensors. Their functionality can also be extended by adding some more elementary structures. The structural construction makes them highly resilient as well, but they are economical, too. In the long run, when some changes have to made in the tensegrity structure, it can be done much easier, with less cost to energy changes [6].

2.4 Disadvantages of Tensegrity Structure

The first disadvantage is that when structures become too large, it would be possible for congestion. Congestion effects happen when the struts run into one another or end up touching one another. This could even result in a high amount of deflections as well. Low material efficiency is possible when they are used across conventional continuous structures. While many functions are supported in tensegrity, there are disadvantages because of how the fabrication forms and technology have not caught up. Fabrication complexity still exists, and because of this, there could be barriers in how they can be developed. With fabrication complexity, when different tensegrity components are created separately, their integration would become a problem.

Another issue resulting from the fabrication technology is how floating compression techniques cannot be created as such. Now in the development of newer tools such as the Tensegrity 2000, high-density structures could be created, but then even these cannot stand loads that over the critical limit. In comparison to conventional techniques, it can bear loads better, but there are some critical limits for the amount of load it can bear [6].

2.5 Application of Tensegrity Structure

Tensegrities are attractive solutions for controllable and smart structures as often; small amounts of energy is needed to change the shape of tensegrity structures [20]. In the broader sense, even, the entire universe can be understood as a tensegrity structure. At a microstructural level, planetary systems or even atomic systems are arranged, while connected with the tensional gravitational force. This constitutes the tensile member forces. What's more, researchers like Snelson [8] describes tensegrity as more of a closed system. "Research into active control of tensegrity structure was initiated in the mid-1990s even biological systems such as cells, tissues, and organ systems can be considered as tensegrity structures. The muscular-skeletal system is also a tensegrity structure. In the technological sector, tensegrity is widely used in building constructions, structures etc.

Architects all over the world make use of the construction technique where they rely on the weight and continuity in stresses for holding. Holding is an important concept here, and weight/continuity of stress combined helps in the holding effect. As an example, consider how a stone dome or a bridge is pulled into place with some tensile forces. The tensile forces that act on the structure result in compressive continuity that both act downward in the structure and also be in charge of sustaining the load. This is how normal architecture is constructed. In the case of tensegrity architecture, it so happens that the principle of tension continuity and compression discontinuity is considered as a system of equilibrated omnidirectional stresses [21] The tensegrities are presented as not needing any support at all and are self-calibrated and pre-stressed.

In the field of aerospace where there is a growing need for aircraft to fly effectively while operating in aerodynamically different regimes, thus demand for wing morphing technologies. Pietila and Cohen developed a dynamic modeling method in [22] that maintains manoeuvring using morphing of airfoil camber without the conventional control surfaces.

2.6 Primary Challenges in Tensegrity Applications

There are a few fundamental problems associated with tensegrity structures, and the primary one is the geometry of the structure. The self-stressed equilibrium of the structure is determined by the form-finding method. There are issues of scalability as well, and sometimes there are manufacturing imperfections as well that could affect the active control of the tensegrity structure. Since much of the ideas on tensegrity structures have been developed based on existing identification with nonlinear geometrical behavior, it also follows that the challenges identified are also on the same track.

Firstly, analytical form-finding methods need to be developed. Without the proper analytical form findings methods, it would be impossible to understand high order tensegrity structures. Secondly, form-finding for arbitrary tensegrity structures more often are seen to involve only a little knowledge of structure. This is especially the case with tensegrity structures such as the spheres, cylinders, and more. There are challenges in simultaneous form-finding, also there are constraints in understanding the member length and axial stiffness parameters. Sometimes, the advancement in the context of parameter identification also poses a challenge as well. In form-finding of assemblies, there are difficulties in identifying the known tensegrity units and the unknown tensegrity grids.

CHAPTER 3: METHODOLOGY

In this chapter, we discuss the analysis and experimental methodology. The form-finding method is also covered here. Form finding of the existing tensegrity structure is essential to understand the characteristics of the structure such as strut length and string stiffness. This is needed as part of conducting the experiment because these values would be compared against measurements taken later to understand the impact.

3.1 Form-Finding Methods for Tensegrity Structures

Tensegrities are types of smart structures. Interests in understanding the structures and how they could be actively employed in more current construction works and other designs are driving new development in the field of tensegrity structures. These structures are such that they lack physical connections, each of the compression members need not be physically connected and this leads to synergistic handling of the loads. In the case of tensegrity structures, it could so happen that there is a growing interest in "smart" structures whose shape can be actively adjusted and controlled. The joints of the structure are predictable, and there is a linear response generated across any form of shape. This is especially attractive when deployable structures must be created. This was one of the strong benefits of the tensegrity structures as presented in the previous section. Furthermore, an interest to study these structures has arisen from how they relate to the biology of materials, such as the structure of viruses, the cellular structures and more [17]. To understand how these smart structures could be actively adjusted and controlled, it is first necessary to understand how they are constructed, and form-finding is the first step.

Contrary to developing and optimizing structures using intuition and experimentation, form-finding is the determination of the design of the tensegrity geometrical configuration analytically. The configuration found should also keep the tensegrity structure in a state of equilibrium. Form finding studies have been carried out on tensegrity structures from the early research studies of Fuller and Snelson. The tensegrity structures that they formed were mostly convex polyhedron based. They used this geometric research to understand the existing structure and understand how to formulate newer configurations if possible.

Tensegrity in general, has a different form of scheme from that of the polyhedron it's based on, and some of its underlying characteristics cannot be taken to represent a general population. A form-finding must be done to find the equilibrium state of a tensegrity structure before an assessment could begin.

An example to understand this is the truncated tetrahedron and the expandable octahedron. In both cases, it could be seen that the self-stressed condition of tensegrity differs its geometric shape from that of the polyhedron [17]. It would be necessary to identify some form-finding methods to understand the underlying equilibrium and only then the simplest configuration of the tensegrity could be assessed.

Different form-finding methods for tensegrity structures have been researched by many authors, but specific classification methods corresponding to types of tensegrity structures have still not been proposed holistically. For instance, authors like Connelly and Terrell, Vassart and Morto and more have proposed methods for understanding the form. These methods could be classified into two categories (i) kinematical method and (ii) statical method. Category (i) consists of three methods which are analytical, non-linear and pseudo-dynamic methods. Category (ii) can be further divided into analytical, force density and energy minimization methods. Each of these methods has its advantages and disadvantages.

The force density (defined as force divided by length) is used to convert the non-linear equilibrium equations into a set of linear equations of the nodes. This method has been supplemented by Vassart and Motro's [23] with techniques for obtaining a set of force densities that would produce the required nullity: intuitive, iterative and analytical.

On the other hand, researchers like Connelly and Back made use of an abstract energy method where they applied group representation theory to discover symmetric placements [24]. The energy minimization method produces a matrix the same as the force-density matrix so we will discuss too much on this method.

Researcher Tran and Lee [25] made use of an advanced form-finding of tensegrity structures which is basically a numerical method. In this advanced method, the only information that is required for numerical assessment will be the topology and type of members. This numerical method is hence more satisfactory given that it asks for only specific details pertaining to the outside shape and the form of member location. Once this is known, the form-finding process can start. In this research work, Eigenvalue decomposition is in fact done, and the Eigenvalue decomposition of the force density matrix combines with the single value decomposition of the equilibrium matrix. They are performed iterative and this numeric method of calculation reveals the following results. Firstly, the combined decomposition results in better identification of the nodal coordinates within the system. Force densities are understood better and they also satisfy the rank deficiencies to be understood in the equilibrium matrix of the tensegrity. By performing an interactive decomposition, the form-finding method is less error-tolerant. The numerical examples are more robust for identifying self-equilibrium in tensegrity structures and are useful for understanding other structures. The numerical method of form finding is furthermore suited for simulative experiments and more, as the numerical analysis is more representative in such contexts [17].

Non-linear programming method turns the form-finding into a minimization of a function with respect to the nodal coordinates. If, for example, we define the objective function $f(x, y, z)$ as the negative length of one of the struts. The objective function should be in the feasible region where the sign requirements of axial forces in cables and struts are met. The problem has the form:

$$\text{Minimize} \qquad f(x, y, z)$$

$$\text{Subject to} \qquad g_i(x, y, z) = 0 \; for \; i = 1, \dots, n$$

In the example of the triangular prism shown in Fig. 4, it has 9 cables of length $l_c = 1$ and 3 struts. The bottom three of its six nodes are fixed in place. We denote $c_1, c_2, \dots, c_6$ lengths of the six remaining cables and $s_1, s_2 \; and \; s_3$ lengths of the struts. The non-linear problem for 3-strut prism is formed below:

$$\text{Minimize} \qquad -l_{s1}^2$$

$$\text{Subject to} \begin{cases} l_{c1}^2 - 1 = 0 \\ l_{c2}^2 - 1 = 0 \\ \dots \\ l_{c6}^2 - 1 = 0 \\ l_{s2}^2 - l_{s1}^2 = 0 \\ l_{s3}^2 - l_{s1}^2 = 0 \end{cases}$$

We can then solve the problem to get the final length of struts is 1.468.

3.2 Static Analysis with Dynamic Relaxation method

Tensegrity can be defined as floating compression. It is based on the structural principle that is the ways in which the isolated components are compressed in a state of continual tensions. The meaning of the structure will fail if the cables yield or in the cases of rod buckle. Preload or tension allows the cables to be rigid in tension. There is mechanical stability that enables the members that remain in the tension or compression as the stresses are found to increase according to the structure. The structural member experience is known as the bending moment. These can produce a rigid structure for the mass and the cross-section of the components. The three-rod tensegrity structure is based on the simpler structure. The variations are known as the needle tower. These entail the use of three cables or more than 3 cables that are redefined on the position of the rod.

The dynamics of the tensegrity structure are gaining interest in the research topic in recent times. In general, it has been stated that with the increase in natural frequency, there is an increase in the pre-stress level. It was the investigation that was done based on the tensegrity-based footbridge and it stated that the fundamental frequency is not impacted by the pre-stress level. Research done in the past has showcased that the linearized equation of the motion is the basis of the equilibrium configuration which is used instead of the complete nonlinear dynamic model. Vibration analysis has been classified into many forms and some of the static and dynamic vibration studies that have been conducted with tensegrity are analyzed in the following part of the work.

In the analysis of the tensegrity structures, it has been identified that there are several mathematical models that can be adopted, but only a few would accurately represent the geometrical nonlinearity. The requirements for precision increase even more when the structures are actively controlled. The dynamic relaxation method was first proposed by Barnes in [26], it is an iterative method which applies finite changes to converge to an equilibrium position. The method uses a dynamic equation of motion to calculate the behavior of structures [27]. According to Barnes [26] and Domer [27] The vibration analysis is classified into incremental, iterative and minimization methods. The first two approaches use the matrix formulation of finite elements. In these methods, it is necessary to have nonsingular stiffness matrices. Below we will go into more details of the minimization method which is used in dynamic relaxation. As a vector-based method, the stiffness matrix is not required thus making it easier to accommodate.

The equation takes the following form:

$$P(t) = M\ddot{d} + C\dot{d} + Kd \tag{1}$$

Here, P is load vector, K is a linear stiffness matrix, M mass matrix, and C damping matrix. The node's motion is traced over time until the sum of residual forces in the nodes converges to a finite value. If we define V= vector of nodal velocities, the residual forces $R^t_{i;(x,y,z)}$ in node, i can be calculated by:

$$R^t_{i;(x,y,z)} = M_{i;(x,y,z)}.\dot{V}^t_{i;(x,y,z)} + C_{i;(x,y,z)}.V^t_{i;(x,y,z)} \tag{2}$$

3.3 Dynamic Analysis Using Euler-Lagrange Equations

In this section, we perform dynamic analysis from a Lagrangian point of view. The general idea behind Lagrangian mechanics is introduced. Then dynamic equations of motion of our 3-bar tensegrity prism is developed in detail.

Figure 2 shows a basic tensegrity structure that we adopted for the table application. It is a 3-Strut tensegrity prism (t- prism) consisting of 3 compressive struts and 9 tensile tendons. It is the simplest and therefore one of the most typical members of the tensegrity family. It is believed first exhibited by the Latvian artist Karl Ioganson in Moscow in 1920-21.

We modified the configuration for the table application. As shown in Figure 3, a top view of this kind of structure with a smaller top platform, before the top platform rotating a twist angle α to gain a balanced position of this configuration. A coordinate system is placed in the center of the bottom platform, and the top platform is free to rotate about Z-axis. The top and bottom triangular are equilateral but not equal to each other. This kind of structure is called a semi uniform. The tendon is defined as the portion of the tensile network between the two adjacent ends of struts. We denote the length of the top, bottom and lateral tie as a, b and L_l, respectively. The length of struts is L_s, and the distance between the top and bottom platform is h.

It is pointed out by Kenner, H. that regardless of the height or diameter of the structure, for this kind of tensegrity structure, for a given number n of struts, the twist angle α is constant and is given by the formulation:

$$\alpha = \frac{\pi}{2} - \frac{\pi}{n} \tag{3}$$

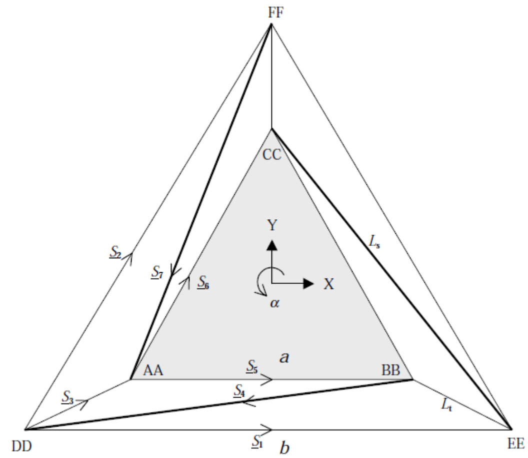

Figure 3:Top View of 3-Strut Tensegrity Prism

Although Kenner's calculation disregarded the tendon stretch and deformation of struts, by making the same approximation, we can still assume that the angle α for our structure to be stable shall be π/6(radius). This can be the static initial configuration of our system. Using all the nomenclature defined before, we have the coordinates of the joints for our table configuration.

$$AA:\left(-\frac{\sqrt{3}}{3}a\cos(\frac{\pi}{6}+\alpha),-\frac{\sqrt{3}}{3}a\sin(\frac{\pi}{6}+\alpha),h\right)$$

$$BB:\left(\frac{\sqrt{3}}{3}a\sin(\frac{\pi}{3}+\alpha),-\frac{\sqrt{3}}{3}a\cos(\frac{\pi}{3}+\alpha),h\right)$$

$$CC:\left(-\frac{\sqrt{3}}{3}a\sin(\alpha),\frac{\sqrt{3}}{3}a\cos(\alpha),h\right)$$

$$DD:\left(-\frac{1}{2}b,-\frac{\sqrt{3}}{6}b,0\right)$$

$$EE:\left(\frac{1}{2}b,-\frac{\sqrt{3}}{6}b,0\right)$$

$$FF:\left(0,\frac{\sqrt{3}}{3}b,0\right)$$

Where α is equal to π/6 as was stated earlier. The endpoints coordinates are used to define the initial configuration of our tensegrity tower.

So we pick a=1 b=2 h=1and α is equal to $\pi/6$ as calculated before. We have:

Node	Coordinates
A	(-0.2887 ,-0.5, 1)
B	(0.5774, 0 ,1)
C	(-0.2887 ,0.5 ,1)
D	(-1 ,-0.5774 ,0)
E	(1 ,-0.5774 ,0)
F	(0, 1.1547, 0)

Table 1: Nodal Configuration

Next, we adopt the Lagrangian's equation to perform a dynamic analysis using the nodal coordinates. In addition, for convenience during analysis, we would like to make some assumptions without loss of generality:

- Lower ends are to remain in the horizontal plane
- Each strut is not allowed to rotation about its longitudinal axis
- The struts are massless.
- All the struts have the same length.
- There are no dissipative forces acting on the system.
- The stiffness of all the top ties is the same.
- The stiffness of all the bottom ties is the same.
- The stiffness of all the lateral ties is the same.
- The free lengths of the top ties are equal.
- The free lengths of the bottom ties are equal.
- The free lengths of the lateral ties are equal.

The coordinates of the joints:

Node	Coordinates
A	$(-\frac{1}{2}a, \frac{\sqrt{3}}{6}a, h)$
B	$(\frac{1}{2}a, -\frac{\sqrt{3}}{6}a, h)$
C	$(0, \frac{\sqrt{3}}{3}a, h)$
D	$(-\frac{1}{2}b, -\frac{\sqrt{3}}{6}b, 0)$
E	$(\frac{1}{2}b, -\frac{\sqrt{3}}{6}b, 0)$
F	$(0, \frac{\sqrt{3}}{3}b, 0)$

Table 2: Generalized Nodal Coordinates

Keep the bottom platform fixed, i.e. joints D, E, and F are fixed, and rotate the top surface. The new coordinates after an alpha degree rotation of the top platform:

Node	Coordinates
A	$(-\frac{\sqrt{3}}{3}a\cos\left(\frac{\pi}{6}+\alpha\right), -\frac{\sqrt{3}}{3}a\sin\left(\frac{\pi}{6}+\alpha\right), h)$
B	$(\frac{\sqrt{3}}{3}a\sin\left(\frac{\pi}{3}+\alpha\right), -\frac{\sqrt{3}}{3}a\cos\left(\frac{\pi}{6}+\alpha\right), h)$
C	$(\frac{\sqrt{3}}{3}a\sin\alpha, \frac{\sqrt{3}}{3}a\cos\alpha, h)$

Table 3: Generalized Nodal Coordinates after Rotation

Based on the coordinates above, the length of the string connecting AD, BE, and CF can be acquired respectively:

String	Length Squared
AD	$(-\frac{\sqrt{3}}{3}a\cos\left(\frac{\pi}{6}+\alpha\right)+\frac{1}{2}b)^2+(-\frac{\sqrt{3}}{3}a\sin\left(\frac{\pi}{6}+\alpha\right)+\frac{\sqrt{3}}{6}b)^2+h^2$
BE	$(\frac{\sqrt{3}}{3}a\sin\left(\frac{\pi}{3}+\alpha\right)-\frac{1}{2}b)^2+(-\frac{\sqrt{3}}{3}a\cos\left(\frac{\pi}{3}+\alpha\right)+\frac{\sqrt{3}}{6}b)^2+h^2$
CF	$(\frac{\sqrt{3}}{3}a\sin\alpha)^2+(\frac{\sqrt{3}}{3}a\cos\alpha-\frac{\sqrt{3}}{3}b)^2+h^2$

Table 4: String Length Squared

For a=1, b=2, and with a 30-degree rotation of the top platform, the unstretched spring length: 1.23

Because the 3 upper joints are fixed to a board, and 3 lower joints are fixed to the ground, the components with potential inertia are the 3 strings connecting upper and lower surface. Assuming masses of all components are zeros. We define L is the Lagrangian function, T kinetic energy and V potential energy of the system. For nonconservative force, we have:

$$L=T-V \tag{4}$$

$$\frac{d}{dt}\left(\frac{\partial L}{\partial\dot{\alpha}}\right)-\frac{\partial L}{\partial\alpha}=F \tag{5}$$

$$\frac{d}{dt}\left(\frac{\partial L}{\partial\dot{h}}\right)-\frac{\partial L}{\partial h}=F \tag{6}$$

$$\begin{aligned}V=\frac{1}{2}k(&\sqrt{\left(-\frac{\sqrt{3}}{3}a\cos\left(\frac{\pi}{6}+\alpha\right)+\frac{1}{2}b\right)^2+\left(-\frac{\sqrt{3}}{3}a\sin\left(\frac{\pi}{6}+\alpha\right)+\frac{\sqrt{3}}{6}b\right)^2+h^2}-1.23)^2\\&+\frac{1}{2}k(\sqrt{\left(\frac{\sqrt{3}}{3}a\sin\left(\frac{\pi}{3}+\alpha\right)-\frac{1}{2}b\right)^2+\left(-\frac{\sqrt{3}}{3}a\cos\left(\frac{\pi}{3}+\alpha\right)+\frac{\sqrt{3}}{6}b\right)^2+h^2}\\&-1.23)^2+\frac{1}{2}k(\sqrt{\left(\frac{\sqrt{3}}{3}a\sin\alpha\right)^2+\left(\frac{\sqrt{3}}{3}a\cos\alpha-\frac{\sqrt{3}}{3}b\right)^2+h^2}-1.23)^2\end{aligned} \tag{7}$$

$a = 1, b = 2$, we get:

$$L = -\frac{1}{2}k(\sqrt{\left(-\frac{\sqrt{3}}{3}a\cos\left(\frac{\pi}{6}+\alpha\right)+1\right)^2 + \left(-\frac{\sqrt{3}}{3}\sin\left(\frac{\pi}{6}+\alpha\right)+\frac{\sqrt{3}}{3}\right)^2 + h^2} - 1.23)^2 \tag{8}$$
$$-\frac{1}{2}k(\sqrt{(\frac{\sqrt{3}}{3}\sin\left(\frac{\pi}{3}+\alpha\right)-1)^2 + (-\frac{\sqrt{3}}{3}\cos\left(\frac{\pi}{3}+\alpha\right)+\frac{\sqrt{3}}{3})^2 + h^2} - 1.23)^2$$
$$+\frac{1}{2}k(\sqrt{(\frac{\sqrt{3}}{3}\sin\alpha)^2 + (\frac{\sqrt{3}}{3}\cos\alpha - \frac{2\sqrt{3}}{3})^2 + h^2} - 1.23)^2$$

$$\frac{\partial L}{\partial \dot{\alpha}} = 0$$

$$\frac{\partial L}{\partial \alpha} = -k\left(\sqrt{\left(-\frac{\sqrt{3}}{3}\cos\left(\frac{\pi}{6}+\alpha\right)+1\right)^2 + \left(\frac{\sqrt{3}}{3}\sin\left(\frac{\pi}{6}+\alpha\right)+\frac{\sqrt{3}}{3}\right)^2 + h^2} - 1.23\right) \tag{9}$$
$$\times \frac{\frac{\sqrt{3}}{3}\left(\frac{\sqrt{3}}{3}\cos(\frac{\pi}{6}+\alpha)+1\right)\sin\left(\frac{\pi}{6}+\alpha\right)\frac{\sqrt{3}}{3}\left(\frac{\sqrt{3}}{3}\sin(\frac{\pi}{6}+\alpha)+\frac{\sqrt{3}}{3}\right)\cos\left(\frac{\pi}{6}+\alpha\right)}{\sqrt{\left(-\frac{\sqrt{3}}{3}\cos\left(\frac{\pi}{6}+\alpha\right)+1\right)^2 + \left(-\frac{\sqrt{3}}{3}\sin\left(\frac{\pi}{6}+\alpha\right)+\frac{\sqrt{3}}{3}\right)^2 + h^2}}$$
$$-k\left(\sqrt{\left(\frac{\sqrt{3}}{3}\sin\left(\frac{\pi}{3}+\alpha\right)-1\right)^2 + \left(-\frac{\sqrt{3}}{3}\cos\left(\frac{\pi}{3}+\alpha\right)+\frac{\sqrt{3}}{3}\right)^2 + h^2} - 1.23\right)$$
$$\times \frac{\frac{\sqrt{3}}{3}\left(\frac{\sqrt{3}}{3}\sin(\frac{\pi}{3}+\alpha)-1\right)\cos\left(\frac{\pi}{3}+\alpha\right)+\frac{\sqrt{3}}{3}\left(\frac{\sqrt{3}}{3}\cos(\frac{\pi}{3}+\alpha)+\frac{\sqrt{3}}{3}\right)\sin\left(\frac{\pi}{3}+\alpha\right)}{\sqrt{\left(\frac{\sqrt{3}}{3}\sin\left(\frac{\pi}{3}+\alpha\right)-1\right)^2 + \left(\frac{\sqrt{3}}{3}\cos\left(\frac{\pi}{3}+\alpha\right)+\frac{\sqrt{3}}{3}\right)^2 + h^2}}$$
$$-k\left(\sqrt{\left(\frac{\sqrt{3}}{3}\sin\alpha\right)^2 + \left(\frac{\sqrt{3}}{3}\cos\alpha - \frac{2\sqrt{3}}{3}\right)^2 + h^2} - 1.23\right)$$
$$\times \frac{\frac{1}{3}\sin\alpha\cos\alpha - \frac{1}{3}(\cos\alpha - 2)\sin\alpha}{\sqrt{\left(\frac{\sqrt{3}}{3}\sin\alpha\right)^2 + \left(\frac{\sqrt{3}}{3}\cos\alpha - \frac{2\sqrt{3}}{3}\right)^2 + h^2}}$$

$$\frac{\partial L}{\partial \dot{h}} = 0$$

$$
\begin{aligned}
\frac{\partial L}{\partial h} = &-k\left(\sqrt{\left(-\frac{\sqrt{3}}{3}\cos\left(\frac{\pi}{6}+\alpha\right)+1\right)^2+\left(\frac{\sqrt{3}}{3}\sin\left(\frac{\pi}{6}+\alpha\right)+\frac{\sqrt{3}}{3}\right)^2+h^2}-1.23\right) \\
&\times\frac{h}{\sqrt{\left(-\frac{\sqrt{3}}{3}\cos\left(\frac{\pi}{6}+\alpha\right)+1\right)^2+\left(-\frac{\sqrt{3}}{3}\sin\left(\frac{\pi}{6}+\alpha\right)+\frac{\sqrt{3}}{3}\right)^2+h^2}} \\
&-k\left(\sqrt{\left(\frac{\sqrt{3}}{3}\sin\left(\frac{\pi}{3}+\alpha\right)-1\right)^2+\left(-\frac{\sqrt{3}}{3}\cos\left(\frac{\pi}{3}+\alpha\right)+\frac{\sqrt{3}}{3}\right)^2+h^2}-1.23\right) \\
&\times\frac{h}{\sqrt{\left(-\frac{\sqrt{3}}{3}\cos\left(\frac{\pi}{6}+\alpha\right)+1\right)^2+\left(-\frac{\sqrt{3}}{3}\sin\left(\frac{\pi}{6}+\alpha\right)+\frac{\sqrt{3}}{3}\right)^2+h^2}} \\
&-k\left(\sqrt{\left(\frac{\sqrt{3}}{3}\sin\alpha\right)^2+\left(-\frac{\sqrt{3}}{3}\cos\alpha-\frac{2\sqrt{3}}{3}\right)^2+h^2}-1.23\right) \\
&\times\frac{h}{\sqrt{\left(\frac{\sqrt{3}}{3}\sin\alpha\right)^2+\left(\frac{\sqrt{3}}{3}\cos\alpha-\frac{2\sqrt{3}}{3}\right)^2+h^2}}
\end{aligned}
\tag{10}
$$

Plug into the Lagrangian equation, we can calculate the equations of motion. As can be seen from the above-deducted equations, the numerical solution for the 3-bar tensegrity structure is rather complicated. For more sophisticated structures, mathematical model complexity increases so would computational power required to solve the equation of motion.

3.4 SimMechanics and Machine Simulation

SimMechanics software is a block diagram modeling environment for the engineering design and simulation of multibody machines and their motions, using the standard Newtonian dynamics of forces and torques. Its latest version comes with Matlab 2019b.

3.4.1 Simulation Sequence

The machine simulation sequence [28] has four major phases, described below. The first two occur before machine motion starts.

1. Model Validation

The simulation first checks data entries from the dialogs and the local connections among neighboring blocks. It then validates the Body coordinate systems; the joint, constraint, and driver geometries; and the model topology.

2. Machine Initialization

The simulation next checks the assembly tolerances of Joints that are manually assembled. The simulation then cuts each closed-loop once, checks all constraints and drivers for mutual consistency and eliminates redundant constraints. It also checks whether a small perturbation to the initial state changes the number of constraints which will lead to violation of the constraints.

3. Force Analysis and Motion Integration

There are four modes of analysis in SimMechanics. Generally, in forward dynamics it applies a given set of force to the bodies to produce accelerations. Then integrates the accelerations twice to yield the velocities and positions. Inverse dynamics starts with a given set of motion and differentiates them twice to yield the forces needed to generate that motion.

4. Stiction Mode Iteration

If stiction is present, the simulation checks at each time step whether the sticky joints transition from one stiction mode to another, then checks for mutual consistency of locked and unlocked sticky joint primitives across the whole model. Non-time-increment simulation steps (algebraic loops) are necessary here.

3.4.2 Modeling Blocks

Although based on Simulink, SimMechanics blocks represent physical bodies instead of modeling mathematical functions. Standard block libraries include bodies, joints, actuators, sensors, and drivers as well as force elements. More blocks are also available such as spring and damper force block which applies a linear damped force between the two bodies. These blocks offer advanced functionalities that facilitate the modeling of complex systems. Details of these blacks will be explained in the next chapter as we move to the model building phase.

3.4.3 Visualization Capabilities

Simscape Multibody visualization window can be open, and models in SimMechanics are displayed as convex hulls during the building and simulation process. This approach is useful for starting to learn how to create complex SimMechanics models. In that case, visualization can be used to guide in assembling the body geometries and connecting multiple bodies. VRML, short for Virtual Reality Modeling Language, is a 3D modeling language used to create physical models. SimMechanics can also be paired with VRML to generate more realistic renderings of bodies.

CHAPTER 4: DEVELOPMENT

In this chapter, the detailed development of the tensegrity structure in the SimMechanics modeling environment is presented. First, the SimMechanics modeling suite is introduced. Next, an initial parameter calculation is provided. Emphasis has been placed on the modeling of string components for the static 5-level tower and strut components as well as a controller for the dynamic tensegrity robot.

4.1 SimMechanics Modeling and Simulation Environment

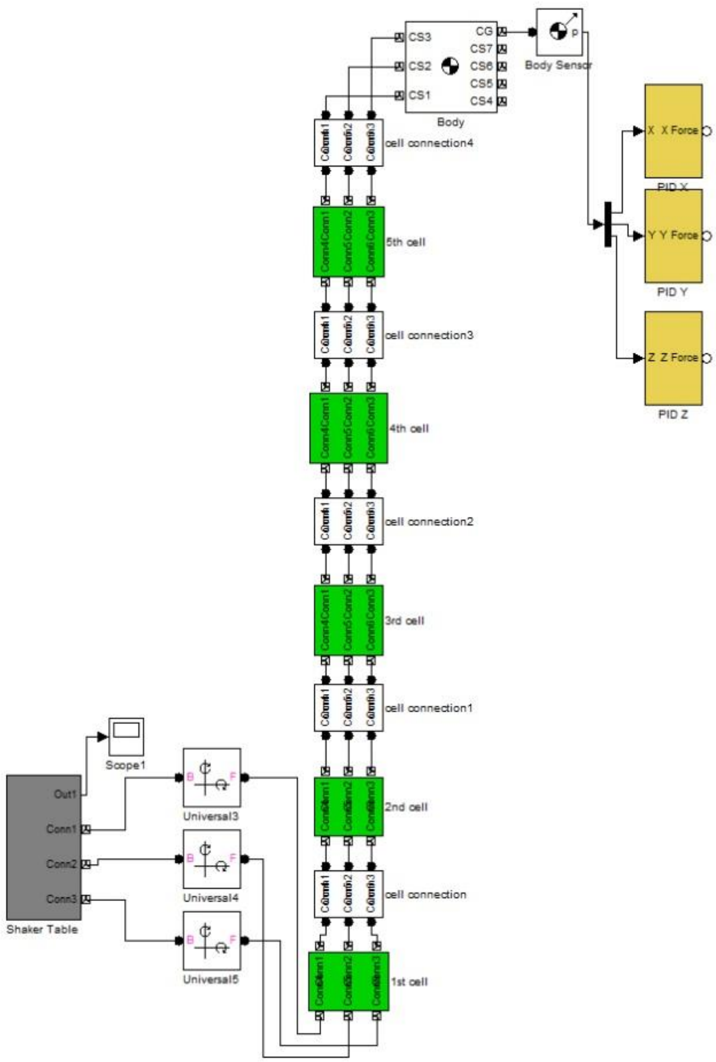

Figure 4: Block Diagram of Five-Layer Tensegrity Tower

Figure 4 shows the block diagram of a 3-strut Five-Layer tensegrity tower in the SimMechanics modeling environment. SimMechanics offers various blocks to define bodies, joints, sensors, and actuators, etc. Different types of blocks have their own properties in order to simulate the actual physical structure. The lines that connect blocks together represent the physical connection between the two blocks instead of data flow as in Simulink [28][29][30].

Body blocks can be defined through mass and inertia properties and local coordinate systems as well. Instead of numerical input, user-defined variables are used for strut properties in order to achieve the easiness of modification during the tuning phase.

Joint blocks are used to constrain the movement between two bodies; they are defined by the type of motion: prismatic or revolute, and reference axis of action. The connecting location of bodies and their attached joint blocks are defined through the body coordinate system. Two of the connected bodies' locations must be aligned for the joint block to work properly.

Both body and joint blocks can be driven by actuator blocks that take conventional Simulink signals and impart torque or force to their attached blocks. Sensor blocks are also available to monitor the body action and output the coordinates, velocity and acceleration measurements for control reference and experimental records. The above blocks allow the embedment of Simulink based controller with the mechanical models which are built-in SimMechanics.

4.2 Static Modeling of Class Two Five-Layer Tensegrity Tower

Tensegrity structures are special cases of tension-trusses. They are built of bars and strings which are attached to the ends of the bars. Members are assigned for special functions: the bars are always axially loaded and resist compressive force while the strings are in tension but can be slack.

In a tensegrity system, each component is either loaded in tension or in compression. As such, cables or springs may be used for the components in tension, thus greatly reducing the inertia and weight of the system. This also allows tensegrity systems to be deployable. Such a system can thus be folded in a small volume for transportation or storage purposes and then be erected into place by tensioning the cables. These attributes make the tensegrity structure a perfect solution for many specific structural requirements. Aside from form-finding, another important issue rising is the design of a tensegrity control system. This chapter looks through a specific type of tensegrity tower (Figure 5). It is constructed by five 3-bar prism tensegrity cells stacking up in the vertical direction. With the ends of struts connected to each other. Sensors and controllers are placed on top of the tower. The visualized structure in SimMechanics is shown in Figure 9.

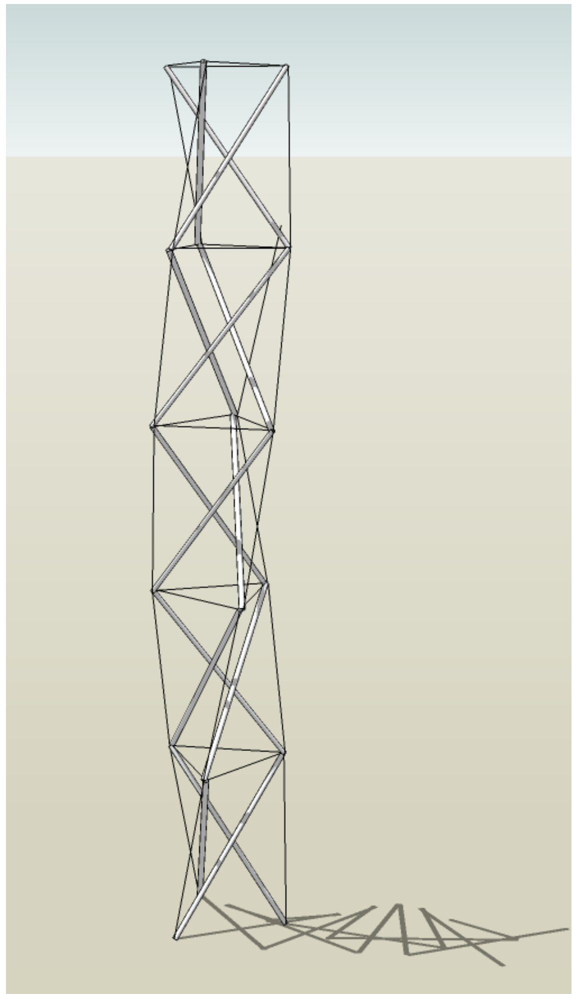

Figure 5: Three-Dimensional Diagram of a Five-layer Tensegrity Tower

4.2.1 String Modeling

A common model of the tensegrity structure's string component was emulated using the spring and damper block that is available from the SimMechanics modeling suite. Such a substitution would be problematic since, instead of taking only tensile load, the spring and damper block can also be compressed like an ordinary spring. The strings are fundamental elements in a tensegrity structure. Thus, to accurately simulate the structure, a user-defined string block was built to replicate a physical string model. This string block will be presented in detail here.

Figure 6 shows the SimMechanics block diagram of a string element. Two body actuators emulate string forces of opposite direction along the string axis. Body sensors are used to observe the coordinate measurements of two ends of the spring for force calculation which is executed in the force block.

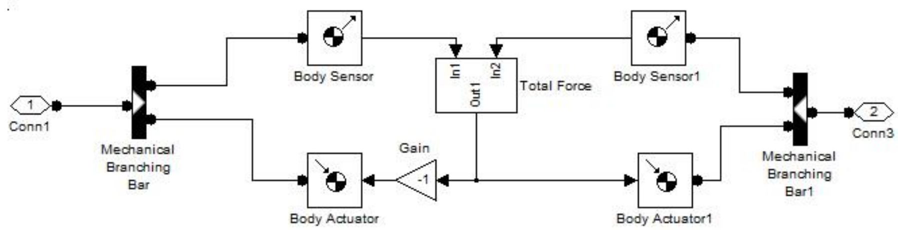

Figure 6: Block Diagram of String Element

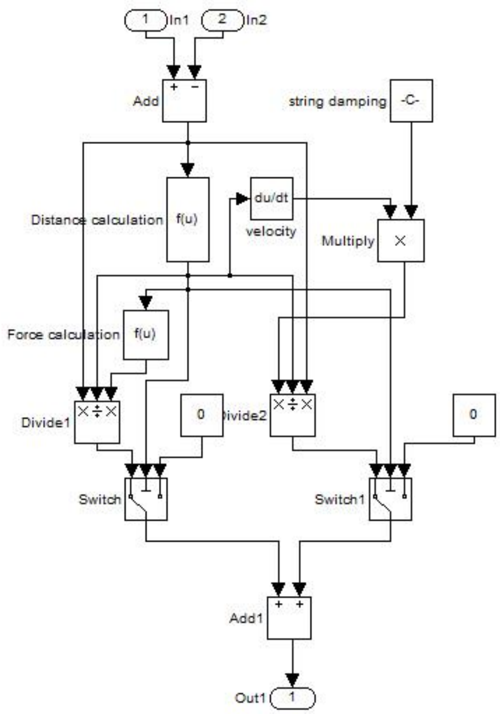

Figure 7: Block Diagram of Force Calculation

The force calculation block diagram is shown in Figure 7. Input position signals are used for distance calculations using the Euclidean distance formula in Cartesian coordinates. The distance between the two ends is first compared to the original length of the string. Unless the spring length is greater than the original length, the spring force calculation should be set to 0 ($F = -kx$). A derivative block is used to calculate velocity. Furthermore, the damping force is determined through: $F = -cv$.

4.2.2 Shaker Table Modeling

The setup of our experiment closely resembled Mr. Chan's presentation at SPIE's 11th Annual International Symposium on Smart Structures and Materials [31]. The structure in the setup was mounted on a shaker table that generated vibration to the bottom stage of the structure. To actuate a physical system modeled by blocks, we need to differentiate an incoming actuation signal. Simulink provides a Derivative block for numerical differentiation of a signal. However, this block's output is sometimes not stable or accurate enough for physical modeling purposes. The SimMechanics User Guide recommends integrator blocks as an alternative to the derivative. Start by specifying the highest derivative signal, such as acceleration, and then integrate this signal to obtain lower derivative signals, such as velocity, using the integrator block.

An alternative is to use a transfer function block, Transfer F_{cn}, to differentiate a signal. This block performs a Laplace transform convolution to smooth the output, which is not exactly the derivative. One may eliminate this drawback by filtering the original signal f, then defining exact derivatives $\frac{dF}{dt}$, etc., of the filtered signal F by adding higher orders to the transfer function numerator.

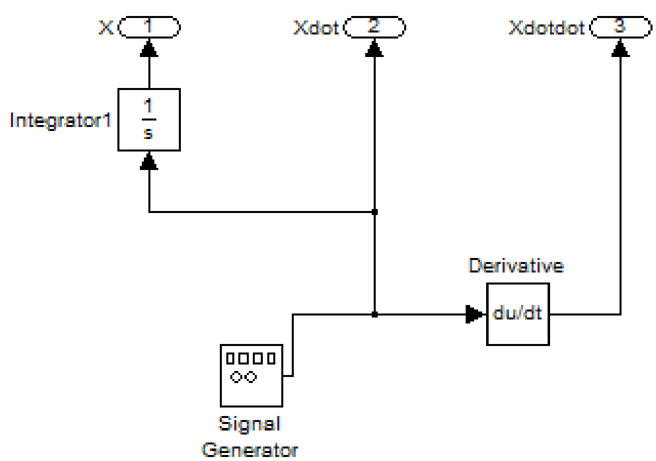

Figure 8: Driver Actuator Signal

In Figure 8, we use both derivative and integrator blocks to generate signals for the driver actuator. The two frames connected to the distance driver should not be placed in the same position in order to avoid the kinematic singularity. As a solution, we recommend setting the position of the follower body, which is the shaker table, to a different position relative to the base body.

4.2.3 Transient Response Simulation

Once we built the SimMechanics tensegrity tower model as shown in Figure 9 animation during simulation, we first carry out the transient response simulation to study the effect string has on settling time. The behavior of the system while approaching the steady-state is called the transient response.

Both string stiffness and damping coefficient are studied. A reference number for string stiffness was obtained from results in research [32]. One kept constant while change the other variable and measurements were taken from sensors mounted at CG of top plate. Stiffness results are shown in Table 5 and Figure 10, for X, Y, Z-axis displacement, respectively. Damping coefficient results are shown in Table 6 and Figure 11, for X, Y, Z-axis vibration amplitude, respectively.

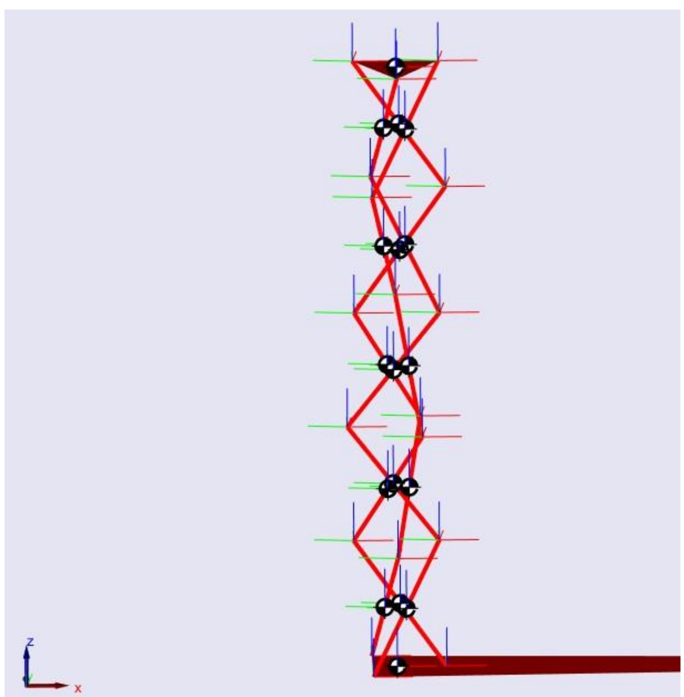

Figure 9: Tensegrity Tower during Simulation

	Ref-1	Ref	Ref+1
String Stiffness (N/m)	30000	50000	70000
String Damping Coefficient (N s/m)	200	200	200
X Settling Time (s)	17	13	11
Y Settling Time (s)	17	13	8
Z Settling Time (s)	11	8	7

Table 5: String Stiffness and Settling Time

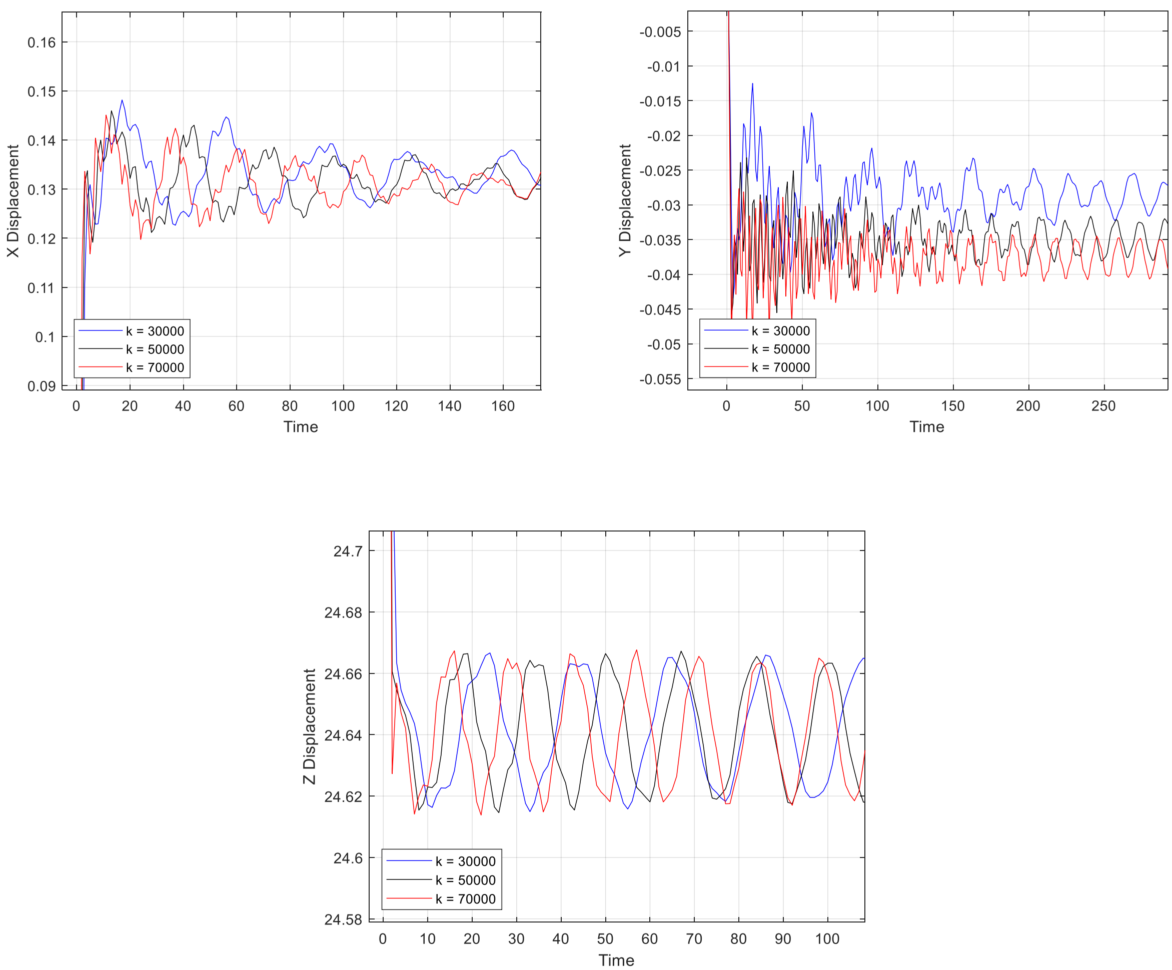

Figure 10: Transient Response Displacement, String Stiffness

	Ref-1	Ref	Ref+1
String Stiffness (N/m)	50000	50000	50000
String Damping Coefficient (N s/m)	100	200	300
X Vibration Amplitude (cm) T=155s	0.71	0.37	0.30
Y Vibration Amplitude (cm) T=155s	0.89	0.40	0.32
Z Vibration Amplitude (cm) T=155s	0.025	0.025	0.025

Table 6: String Damping Coefficient and Vibration Amplitude

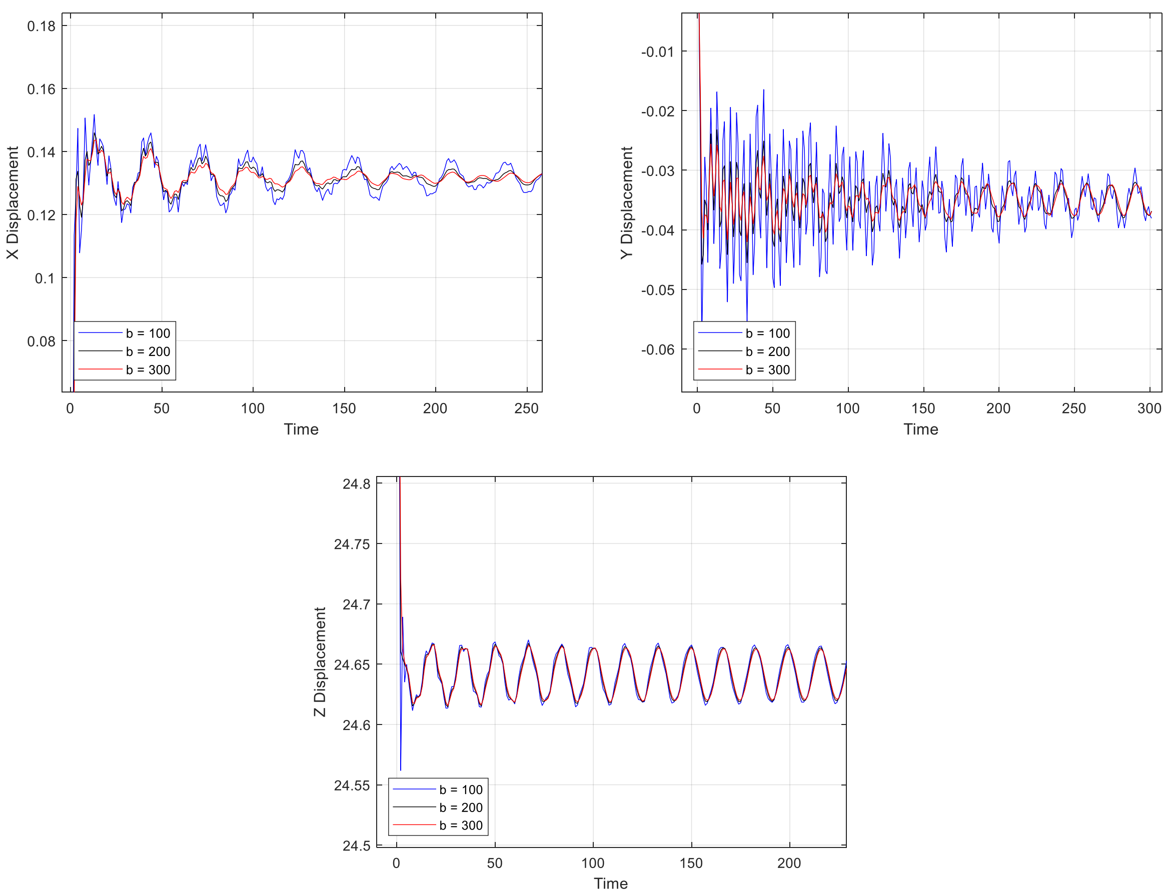

Figure 11: Transient Response Displacement, String Damping Coefficient

4.2.4 Forced Vibration Simulation

Vibration tests were conducted to establish the relationship between string stiffness levels and structure dynamic responses. The **c**hirp signal is used to determine the natural frequencies of the structure [32]. Linear chirp signals, with linearly increasing frequency with respect to time, have strong SNR excitations. Linear chirp signals have, therefore, and become one of the typical signals used in structure modal testing [33] [34]. The linear chirp signal can be expressed as:

$$x(t) = \sin\left[2\pi \int_0^t f(t')\, dt'\right] = \sin\left[2\pi \int_0^t (f_0 + kt')dt'\right] = \sin[2\pi(f_0 + \frac{k}{2}t)t]$$

Where f_0 is the starting frequency (at time t = 0), and k is the rate of frequency increases

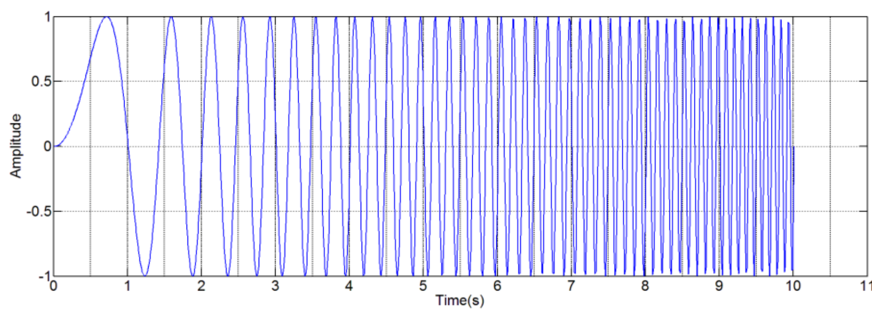

Figure 12: Sample Chirp Signal

The shaker table was excited by a Chirp Signal block in Simulink, which generated a sine wave whose frequency increased linearly with time. Figure 12 shows this sine wave signal; the frequency increases from 0 Hz to 10 Hz over 10 seconds. Sensors were placed on the central top of the fifth stage and the central bottom of the tower to record displacement measurements. The samplings of measurements were 100 Hz, 10 times greater than the maximum vibration frequency of the shaker table. The amplitude peak occurs at the frequency corresponding to the structure's natural frequency under certain string stiffness. Table 7 shows the correlation between string stiffness levels and natural frequencies. These results confirm that, as observed in Ali's paper [20], the dynamic response of the tensegrity structure is closely related to the string stiffness level. Figure 13 is the time history of horizontal displacement of the top plate along the x-axis with a string stiffness 40000 N/m. Figure 14 plots the time history of horizontal displacement of the top plate along the x-axis with a string stiffness 70000 N/m. For comparison, Figure 15 is experimental results extracted from Ali and Smith's research in [20].

	Ref-2	Ref-1	Ref	Ref+1	Ref+2
String Stiffness (N/m)	30000	40000	50000	60000	70000
Natural Frequency (Hz)	3.60	4.13	4.34	4.79	4.99

Table 7: String Stiffness Level and Tensegrity Natural Frequency

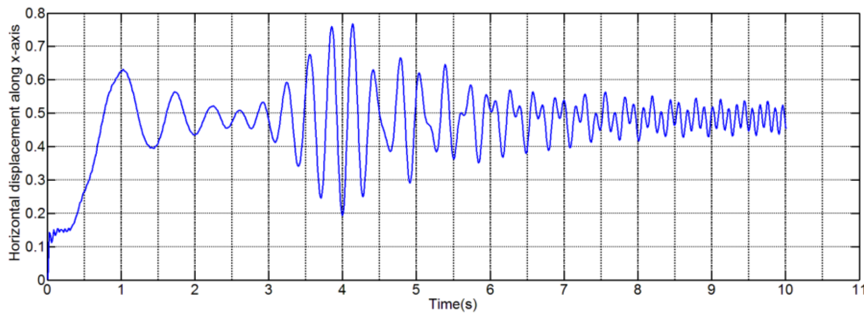

Figure 13: Time History of Horizontal Displacement of Top Plate (String Stiffness 40000 N/m)

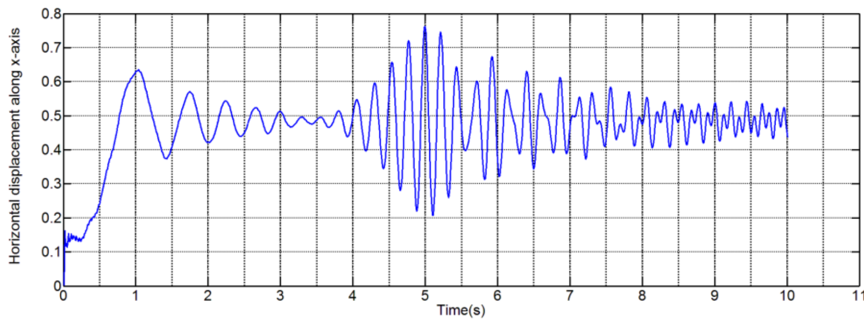

Figure 14: Time History of Horizontal Displacement of Top Plate (String Stiffness 70000 N/m)

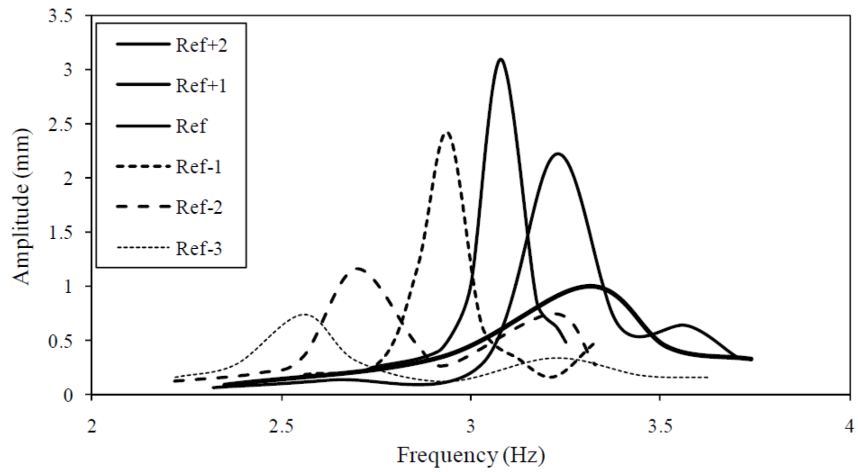

Figure 15：Vibration Amplitude at node 39 for Different Excitation Frequencies and Stress Levels

Source: [20]

4.2.5 Bending Mode Simulation

The object of this step is to explore the accuracy of dynamically modeling tensegrity structure in SimMechanics. Simulation results is compared to experimental results from [31]. Our model was modified into a 3-Layer tower (Figure 18) according to the physical experimental setup. The structure is mounted on a supporting plate which is attached to a shaker table. Sensors are mounted to the top plate and shaker table. They measure the accelerations and displacements of the top and bottom plates.

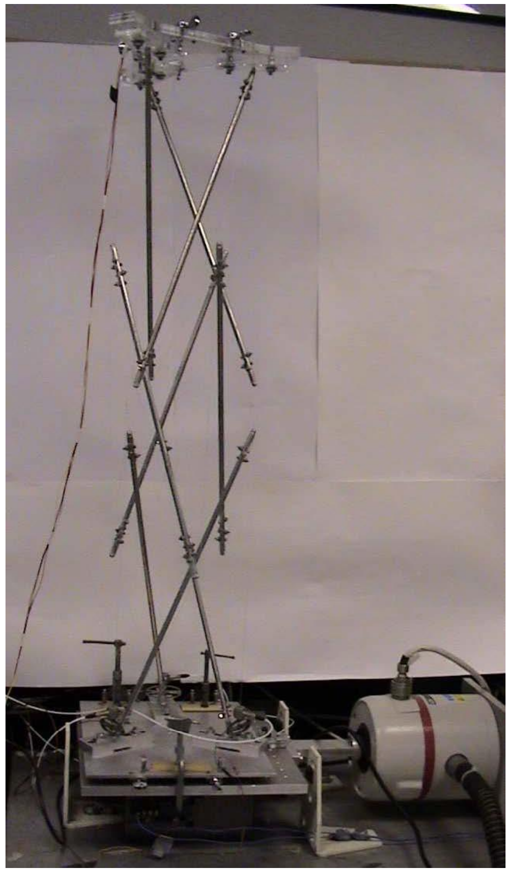

Figure 16: Experimental Setup

Source: [31]

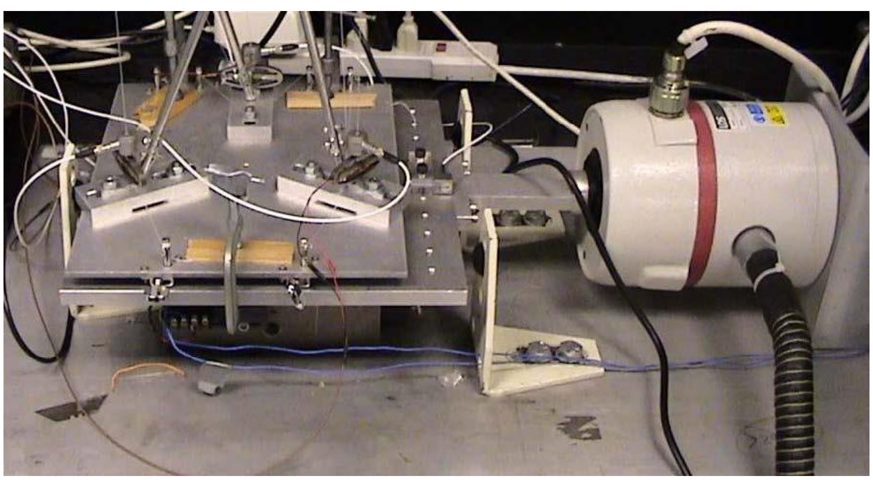

Figure 17: Shaker Table Setup

Source: [31]

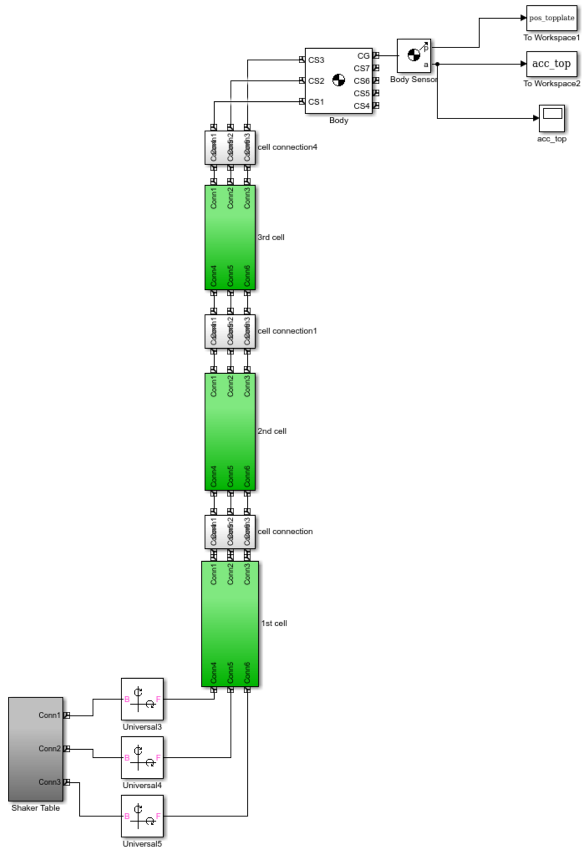

Figure 18: Block Diagram of Three-Layer Tensegrity Tower

For the physical model, the computer generates a band-limited white noise signal to the shaker, which in turn vibrates the structure's bottom. Accelerometers record the acceleration amplitude of the top and bottom of the structure during the vibration.

In SimMechanics, chirp signal ranges from 0 to 40 HZ is used to excite the vibration base. Signal duration is given for 50 seconds to allow enough time for the structure to settle. Measurements were taken from sensors mounted on top and bottom CGs of our model.

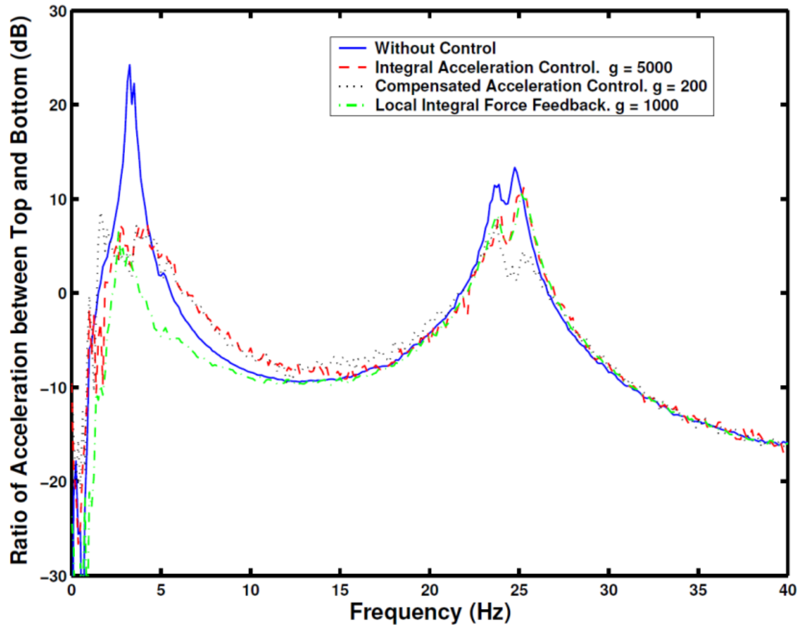

Figure 19: Acceleration Ratio between Top and Bottom Plate(dB) vs Frequency (Hz), Physical Model

Source: [31]

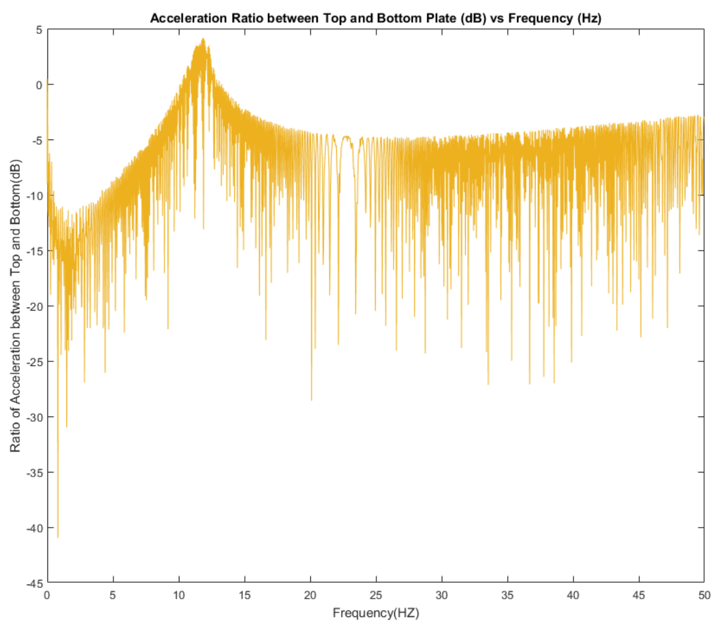

Figure 20: Acceleration Ratio between Top and Bottom Plate(dB) vs Frequency (Hz), SimMechanics Model

4.2.6 Interpretation of Experimental Results

This static simulation presents a detailed tensegrity structure modeling method in the SimMechanics environment. A complete model of a 5-stage tensegrity tower was built to verify this modeling method.

In transient response simulation, two main observations were made. Firstly, it was clear a negative correlation existed between structure settling time and string stiffness. Secondly, vibration amplitude and string damping are also negatively correlated.

In forced vibration simulation, it can be seen from Table 7, structure natural frequency increases with respect to the level of self-stress. The results conform with both modal analysis and vibration experimental results found in [20].

In bending mode simulation, our model in SimMechanics exhibited similarities with the physical model in terms of the ratio of acceleration between the top and bottom plates. The research team constructed the physical model at UCSD and more details of their research can be found in [31]. Our results indicated one bending mode which occurs at the frequency of 12.5 HZ, while the results from [31] indicate two damping modes occur at around 5 HZ and 25 HZ. Two factors possibly cause a difference in results. Firstly, as can be seen in Figure 16, the model from [31] is constructed in a way that the middle cell has their lower struts placed in the middle of the lateral strings of the lowest cell, so is the way top cell stacks on the middle cell. The way this tower is constructed is a class-1 tensegrity structure where at each node, there is a maximum of 1 strut connected. In our SimMehcanis model, however, we have lower nodes of the middle cell connected directly with upper nodes of the lower cell and same connection with top and middle cell, as shown in Figure 9. Our configuration is called a class-2 tensegrity structure. So there exist differences in the ways cells are connected. The reason is, in SimMechanics, the string block is modeled as force element. While the spring blocks can be used to actuate body blocks, there can not be any physical connection between the two. Secondly, we were not able to obtain exact specifications of the model from [31], so guesstimation was used to define some of the physical properties of our SimMechanics model. This also contributed to the discrepancy in experimental results.

The simulation results indicate that a computational modeling and researching approach is accurate enough to reflect the physical model characteristics of tensegrity structures. This section lays a foundation for dynamic control research, which will be presented below.

4.3 Dynamic Modeling and Control Simulation

We further explore the SimMechanics modeling capabilities of the tensegrity structure in the dynamic control field. In [35], Jones and Cohen applied fuzzy logic control to investigate the behaviour of a tensegrity-based UAV morphing wing. In this section, a simple 3 struct tensegrity robot (Figure 21) is constructed in SimMechanics. To verify the feasibility of using tensegrity structure as mobile robotic application, compressed components have been modeled as linear actuators and the PID control algorithm has been devised. The control is carried out by adjusting the length of each strut, and the discussion presents the model characteristics and discusses the algorithm that goes along with the characteristics. The goal of this section is to study the vibration and control characteristics of a tensegrity structure. As part of achieving this goal, the following objectives are presented:

- To explore the feasibility of tensegrity in mobility robot
- To build a tensegrity robot in SimMechanics that would be useful for determining form and for testing different control strategies

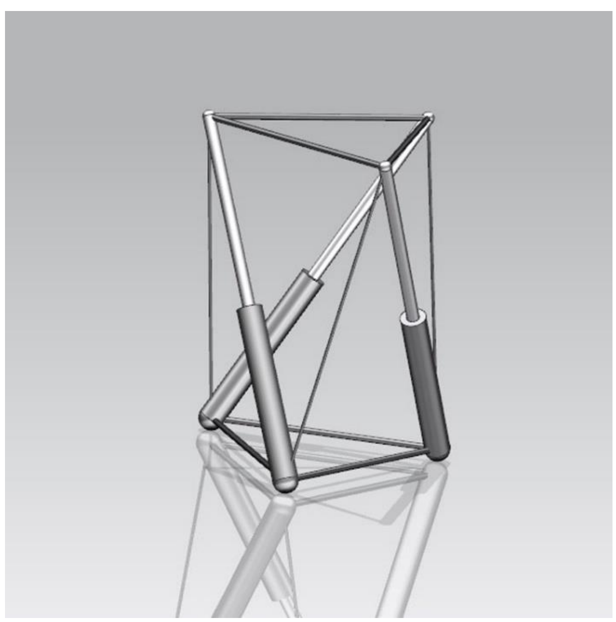

Figure 21: 3-Strut Tensegrity Robot

4.3.1 Model Parameters

The struts are modeled as pipes made of aluminum. Their material denotation is aluminum 6061. The density of the aluminum is 2800 kg/m^3. The outside diameter of the struts is 0.28m, and their thickness is around 0.4m, the upper strut volume is 0.2535 m^3, and the top plate mass is 50kg. AutoCAD modeling tool has been used to find out the Struts moment of inertia.

Lower struts inertia tensors:		
1.0e+03 *		
3.7136	0.5747	2.4353
0.5747	6.2481	0.8295
2.4353	0.8295	2.9285
1.0e+03 *		
5.1168	-1.3848	-1.936
-1.3848	4.8448	1.6943
-1.936	1.6943	2.9285
1.0e+03 *		
6.1121	0.8102	-0.4993
0.8102	3.8495	-2.5238
-0.4993	-2.5238	2.9285
Upper struts inertia tensors:		
1.0e+04 *		
2.4842	0.0013	0.0056
0.0013	2.412	0.5552
0.0056	0.5552	0.1903
1.0e+04 *		
2.4289	0.0306	-0.4836
0.0306	2.4673	-0.2728

-0.4836	-0.2728	0.1903
1.0e+04 *		
2.4312	-0.0319	0.478
-0.0319	2.465	-0.2824
0.478	-0.2824	0.1903

Table 8: Struts Moment of Inertia

The static configuration parameters are presented here. The goal of the experiment is to define the right configuration parameters to get the model to behave as close as possible with the real physical model.

4.3.2 Tensegrity Robot Modeling

A complete overhaul of the previous built SimMechanics model was needed to allow for actuator and control input. As shown in Figure 22 complete block diagram of the newly built 3-strut tensegrity robot.

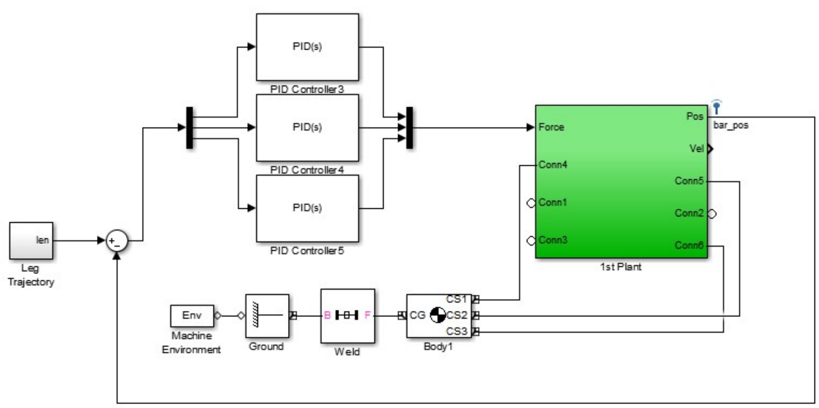

Figure 22: Block Diagram of 3-Strut Tensegrity Robot

Three lower nodes are fixed to the ground with universal joints. The struts have an upper and a lower part and will be linked together with an actuator as can be seen in Figure 23. The actuator is linear and cylindrical, which resembles hydraulic actuators in real life. Control signals are applied to enable each strut to extend or retract independently to achieve the desired top plat position and attitude.

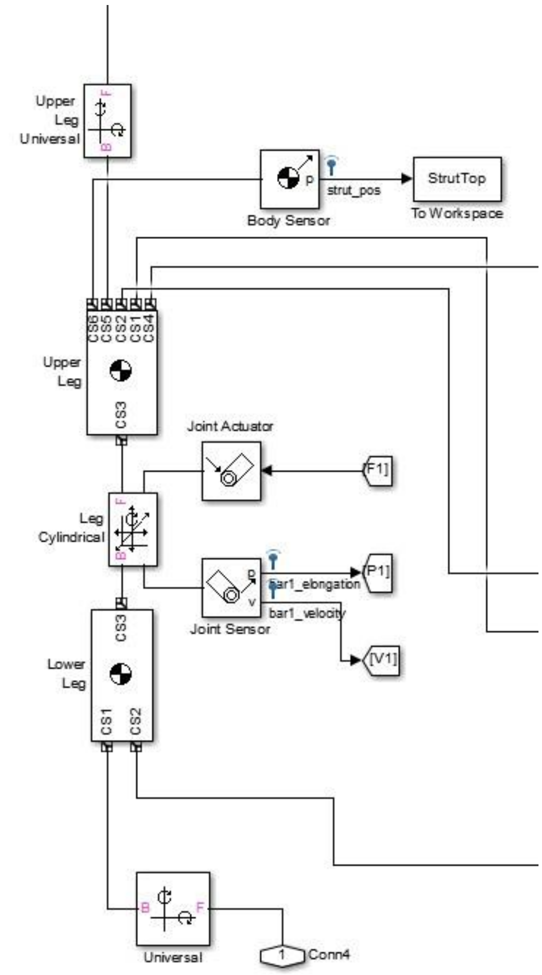

Figure 23: Block Diagram of Strut

For strings components, we will have to consider whether the tensegrity structure becomes unstable when strut length is changed from an initial setting. Then secondly, the springs are used to replace string blocks in the simulation since they can passively change to required lengths.

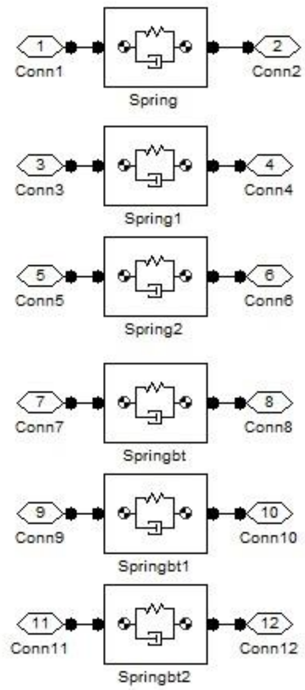

Figure 24: String Blocks of Tensegrity Robot

Finally, Leg length trajectory calculation control error for each leg length:

|| (R*p_t + p) - p_b || - ln

where R is the Euler rotation matrix for the top plate, p is the desired position of the origin of the top plate, p_t is the leg attachment point at the top plate. p_b is the leg attachment point at the base, l_n is the nominal strut length. The block diagram is shown in Figure 25.

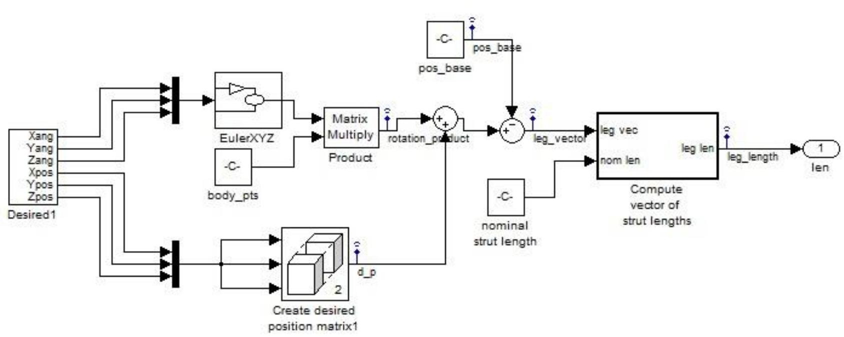

Figure 25: Block Diagram of Leg Trajectory

The leg length trajectory are then calculated. The control error for leg length is calculated as a function of R and p, where R is the Euler rotation matrix, and for the value of the top place, p is considered as the desired position of the origin of top place and the leg attachment point is considered as well in the calculation. Figure 26 shows the tensegrity robot during SimMechanics simulation.

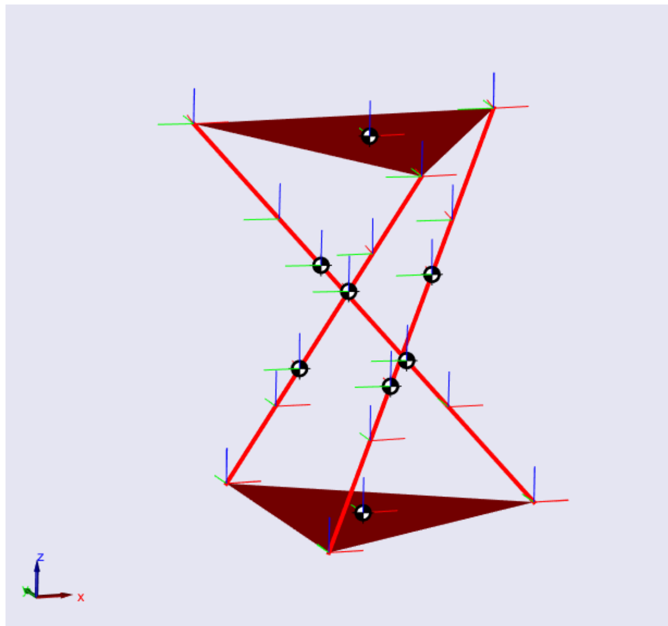

Figure 26: Tensegrity Robot during Simulation

4.3.3 Transient Response Simulation

Transient responses of the model from the initial setup are shown in Figure 27. As shown in the results, the initial height of 10.5948 from our Tensegrity form-finding calculation is not maintained due to spontaneous structure rotation. The structure is unstable when the controller is not engaged. In the next section, we will introduce the PID feedback controller to our model and then proceed to fine-tuning model parameters. Measurements of position and velocity are taken from the cg of the top plate.

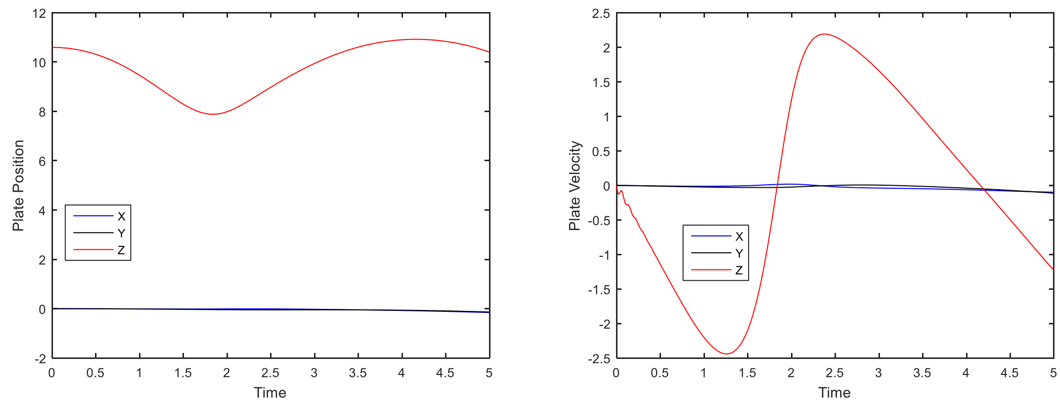

Figure 27：Transient Response w/o Controller

4.3.3 PID Controller and Model Tuning

The control strategy we applied is a classic feedback controller. The PID classic feedback controller (Figure 28) is utilized as a motion controller for the experiment's first stage. To achieve optimal performance, the PID controller needs to be tuned. In this section, for simplicity reason, we will employ the Matlab build-in PID Tuner app (Figure 29) to help tune the gains of the controller. As tuner is for single input single output (SISO) signals, and our model is symmetric along Z axis, we can tune for one controller and duplicate the results to the other two controllers. The transient strut response after tuning is shown in Figure 30. We can see that the tuned PID controllers were able to maintain structure in its initial configurations quiet well. For all the simulations below, the PID controller is engaged with the following parameter settings:

- PID gains: $K_p = 3.54 \times 10^6$; K_i=4.67×10^6; $K_d = 1.98 \times 10^5$
- PID reference input: angles: $\mathrm{X} = \mathrm{Y} = \frac{\pi}{2}, Z = 0$
- PID reference input positions: $\mathrm{X} = \mathrm{Y} = 0, Z = \text{Total height } (10.5948)$

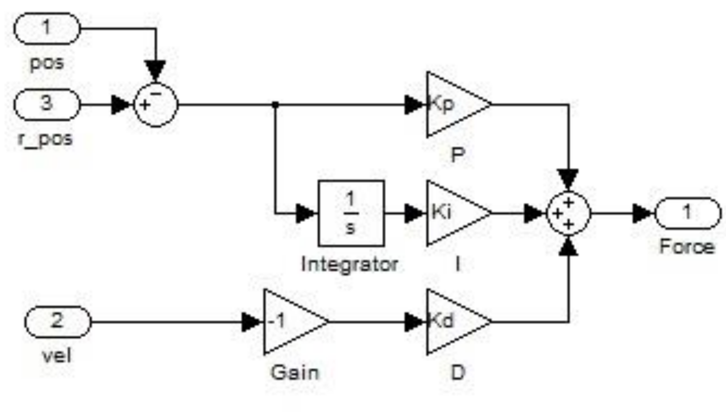

Figure 28: PID Controller Diagram

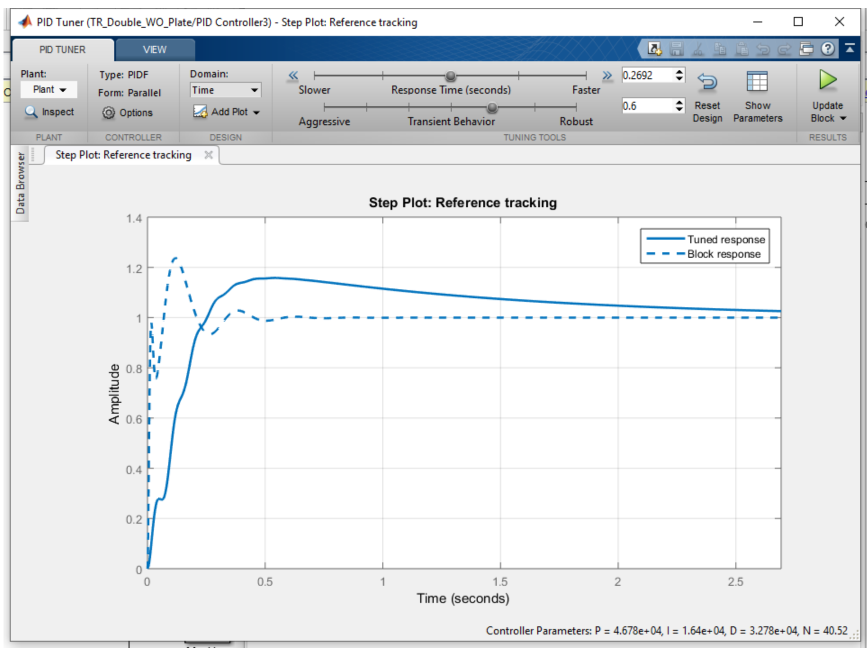

Figure 29: Matlab PID Tuner Interface

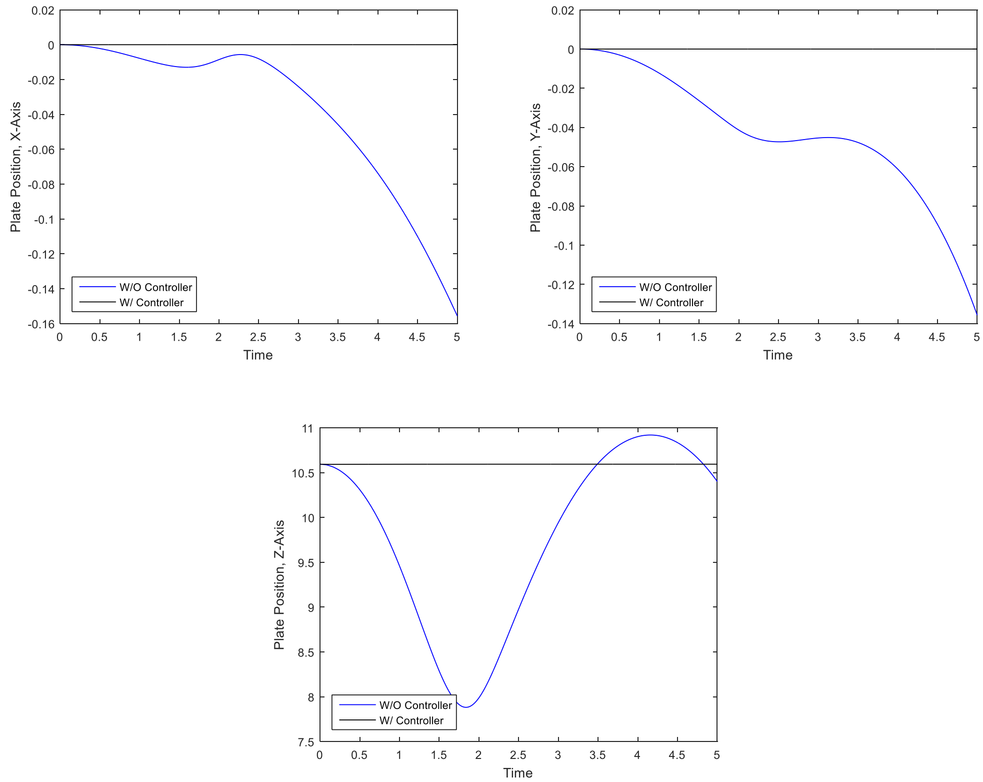

Figure 30: Transient Response w/ Controller

Next, we will study the correlation between string parameters and the model transient response. Our goal is to configure the structure with correct string parameters that best represent real physical models. String parameter selection is shown in Table 9. Set S1-S4 are used to study the effect of string natural length has on transient response. Once an ideal natural length is determined, set S5-S7 are selected to explore how string stiffness and damping coefficient affect the model response. Simulation results are plotted in Figure 31-34.

Set	Longitudinal String Natural Length (m)	String stiffness (N/M)	String damping coefficient (N s/m)
S1	Strut length -1	5×10^6	1.5×10^4
S2	Strut length -1.5	5×10^6	1.5×10^4
S3	Strut length -2	5×10^6	1.5×10^4
S4	Strut length + 1	5×10^6	1.5×10^4
S5	Strut length -1.599	5×10^6	1.5×10^4
S6	Strut length -1.599	9×10^6	1.5×10^4
S7	Strut length -1.599	9×10^6	6×10^4

Table 9: Static Configurations for Initial Setup

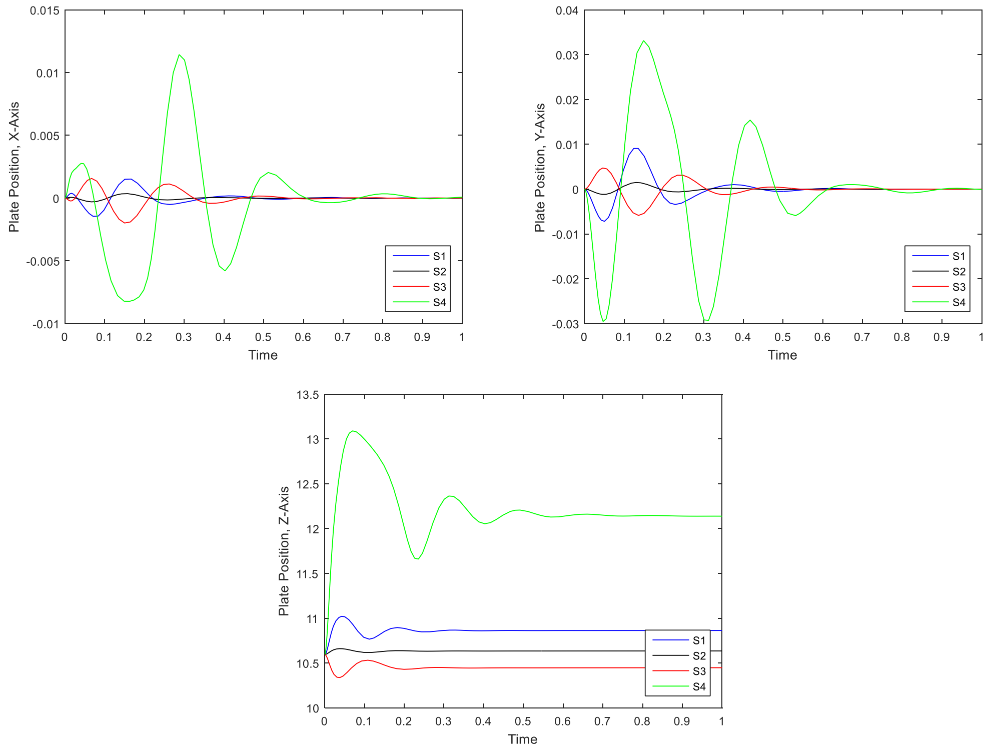

Figure 31: Set S1-S4, Position

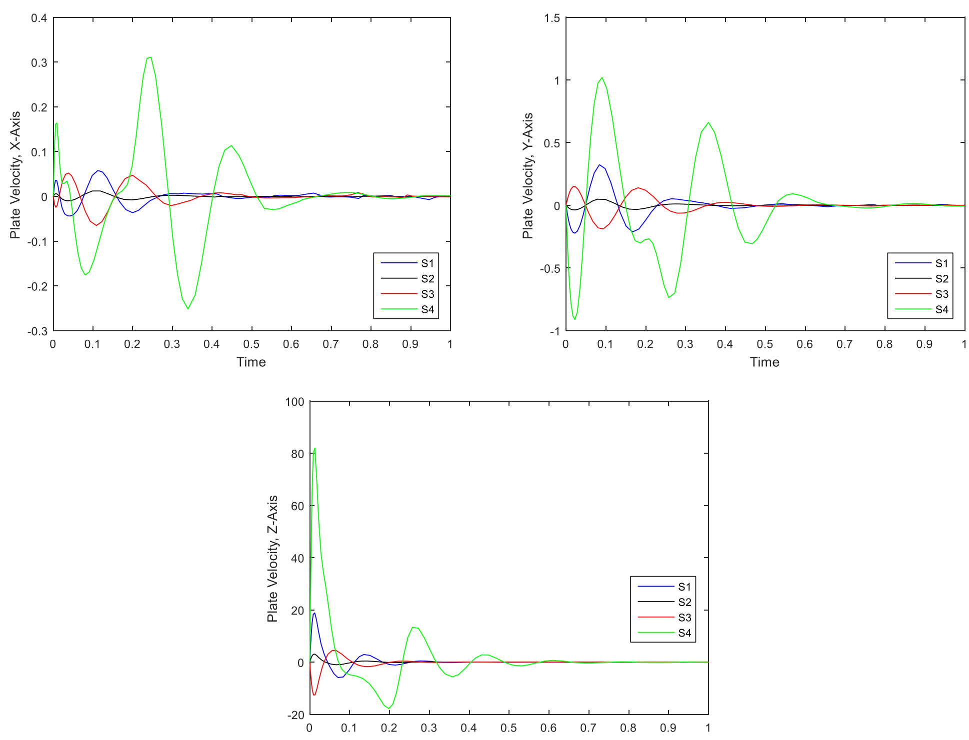

Figure 32: Set S1-S4, Velocity

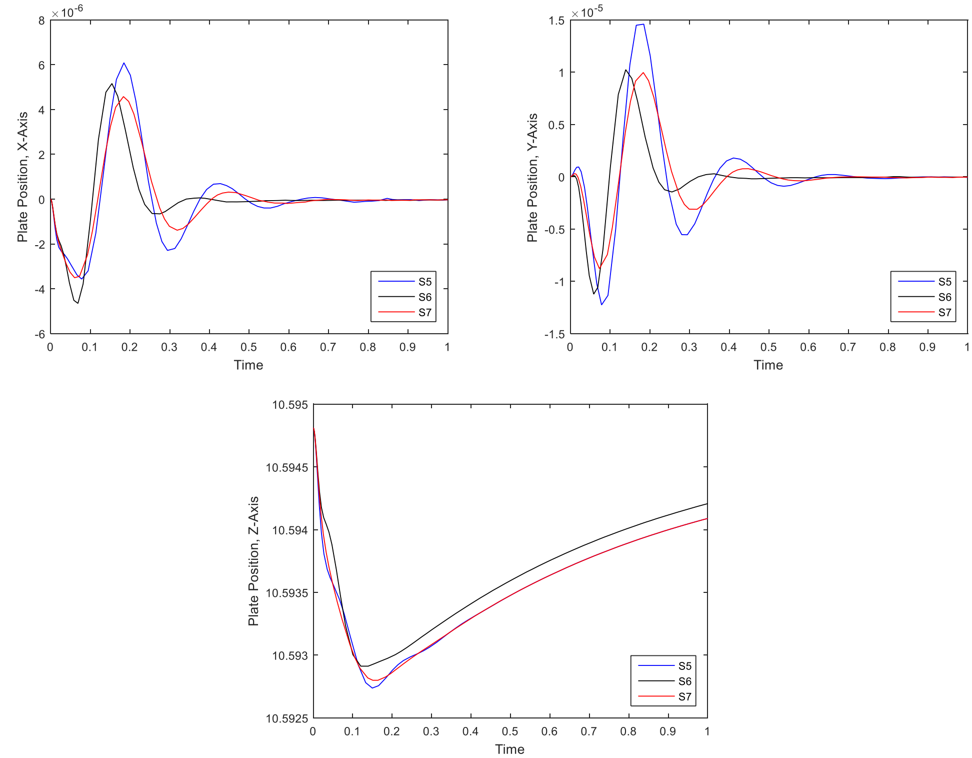

Figure 33: Set S5-S7, Position

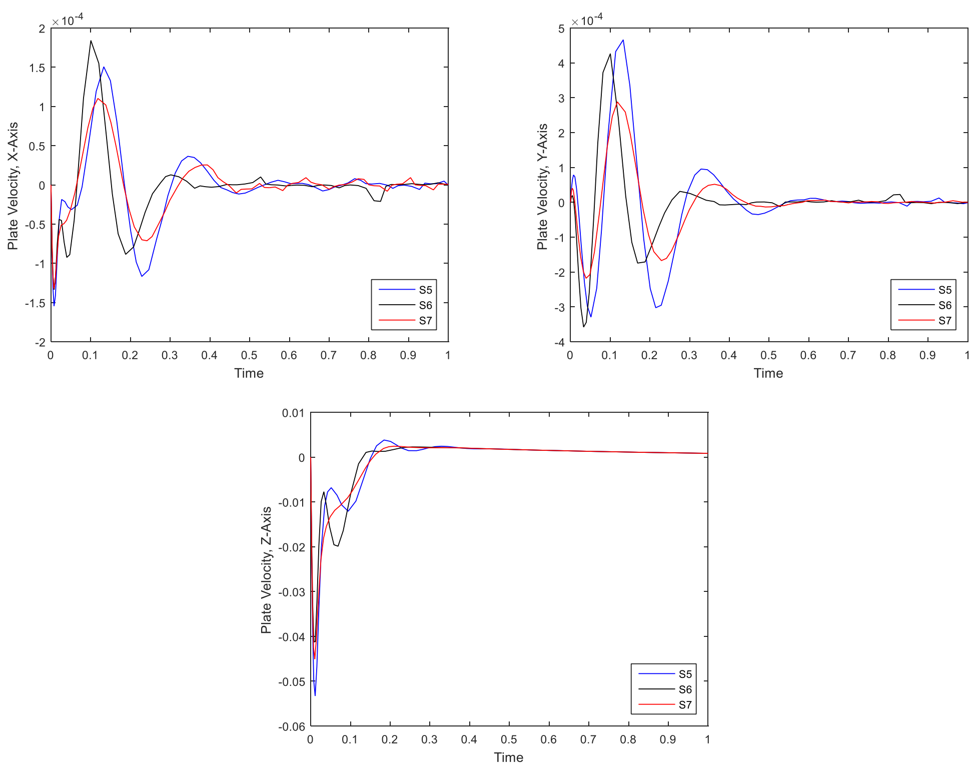

Figure 34: Set S5-S7, Velocity

From the above results, we have come to the following conclusions:

- The initial height is mainly relevant to longitudinal string natural length (L), a carefully tuned initial length will be able to set the tensegrity z-axis displacement as close as to its initial settings (0-degree spontaneous rotation). Let's call this length L_i (L_i is around the length of Strut length-1.6)
- The effect of the longitudinal string natural length also exists in tensegrity robot structure stability. If strut length> L >L_i, as L approaching L_i, the magnitude of oscillation for both position and velocity decreases, indicates an increase of stability within the structure. If L < L_i a decrease in structural stability.
- When we set L > strut length (S4), we observe the structure was unable to maintain a tensegrity prism setting because of a near 240degree rotation. Keep in mind this is because since we replaced string members with spring, when L >strut length, the spring member is in compressive condition; thus the structure does not qualify as tensegrity.

Effects of string stiffness (K) and damping coefficient (C):

For Exp. S5-S7, using the conclusion derived previously, the string natural length has been set to 12.7381 so that the structure can maintain the initial height after settling (no spontaneous rotation).

- From simulation S5- S7, we can observe that increased string stiffness (K) also helps compensate the spontaneous rotation from the initial configuration, although the effect is merely observable compared to those from the change of longitudinal string natural length

- The main effect of increasing string stiffness and damping coefficient can be seen as a decrease in the magnitude of oscillation of both displacement and velocity.

- From simulation S6-S7, the increasing of damping coefficient (C) also helps reduce the settling time of the structure from the initial configuration.

4.3.4 Dynamic Control Simulation

In this section, we explorer model response in the dynamic control fields, which is taking a tensegrity structure from its rest position to a desired one by controlling the length of its strut(s). These types of simulations are desirable in the tensegrity robotics research field. For control response, a step input in the magnitude of 1 is applied at simulation time 1 sec. We place the input signal in the “Desired block,” which is located on the left side of the leg trajectory block diagram (Figure 25). The diagram is shown in Figure 35, notice, Z-axis step input is added to the initial height. X,Y, and Z positions are plotted separately in Figure 36-38.

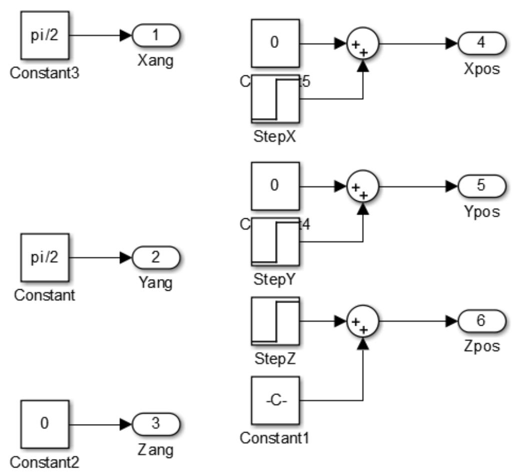

Figure 35: Step Input Diagram

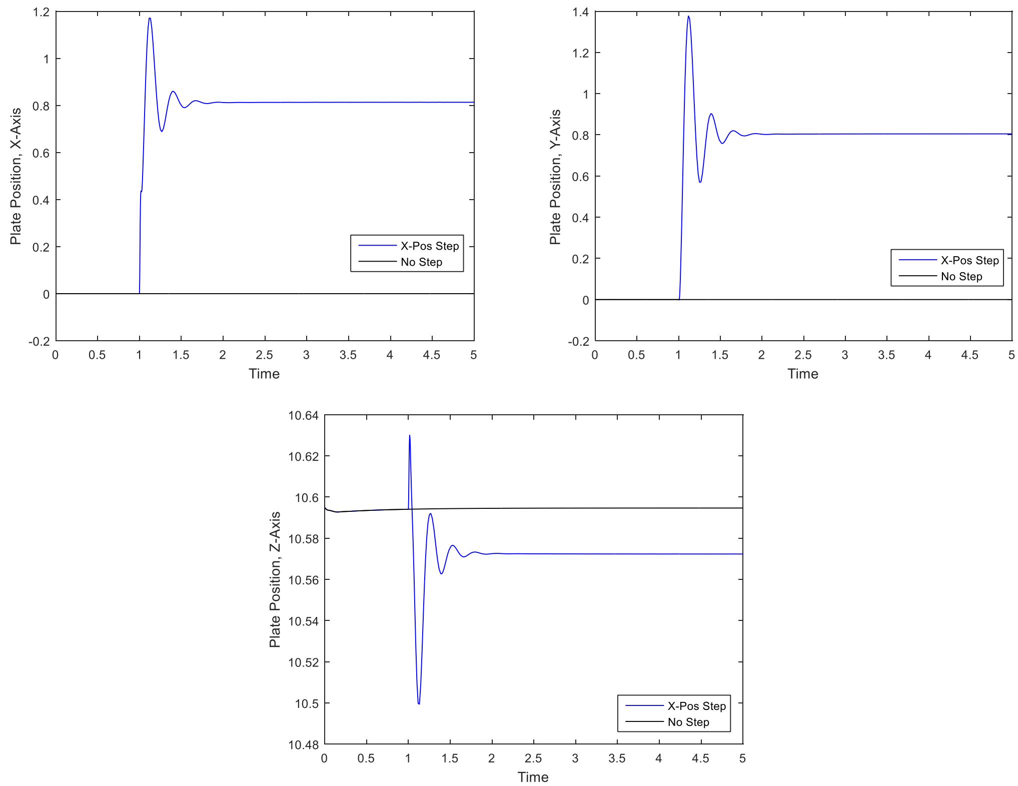

Figure 36: X-Axis Step Response

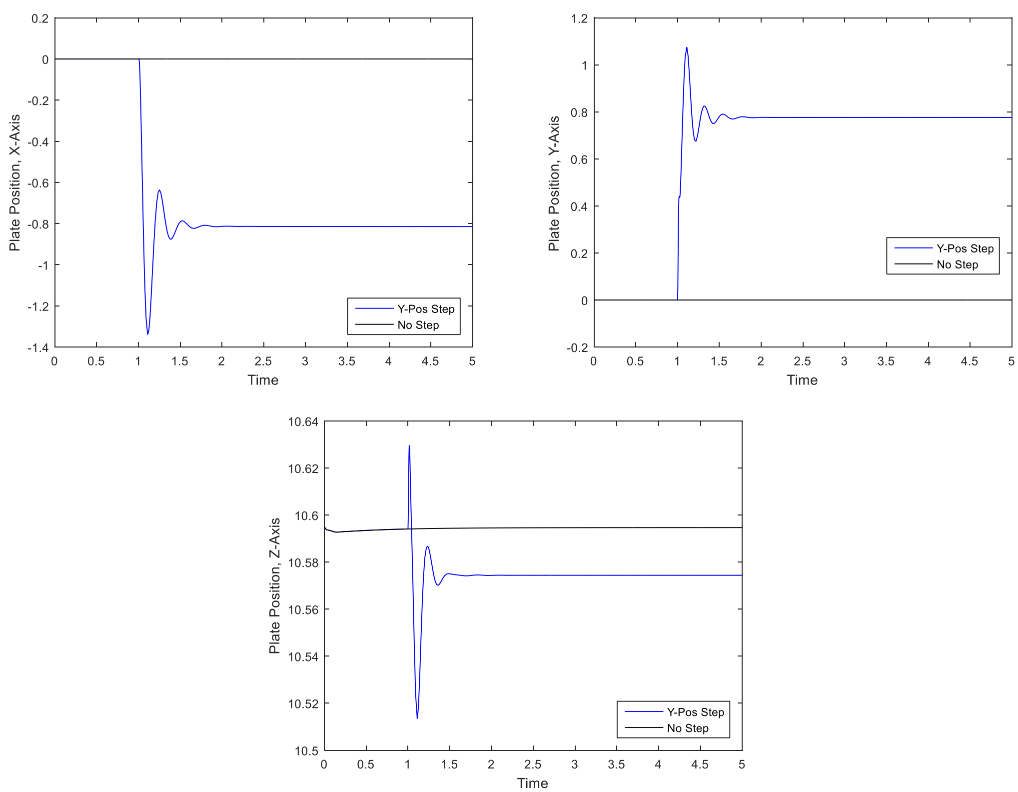

Figure 37: Y-Axis Step Response

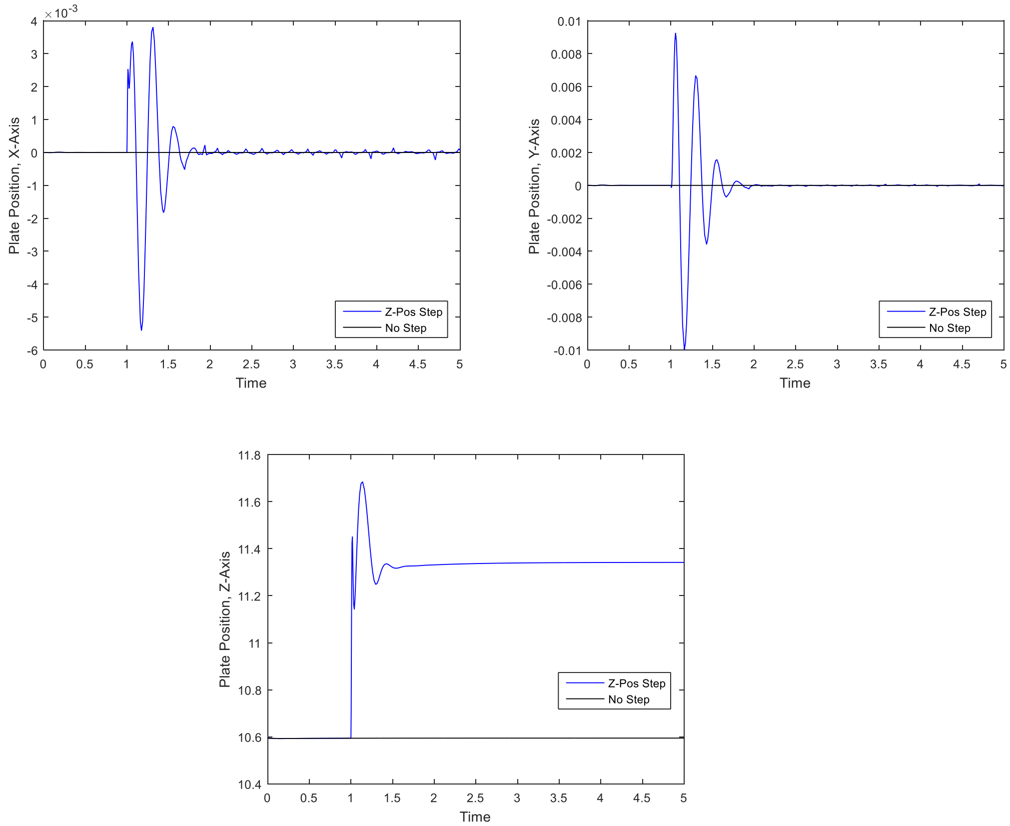

Figure 38: Z-Axis Step Response

The controller force input of each strut for each step response are plotted in Figure 39-41; each plot has been enlarged to the right for ease of reading.

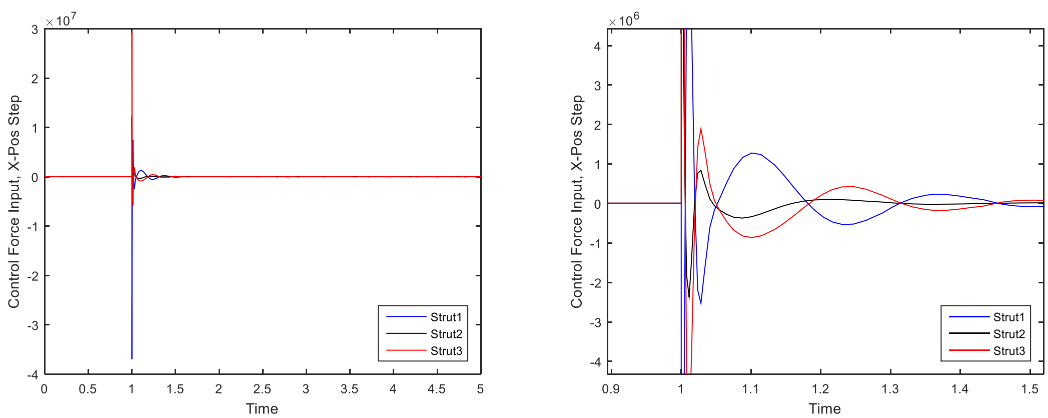

Figure 39: Control Force Input, X-Pos Step

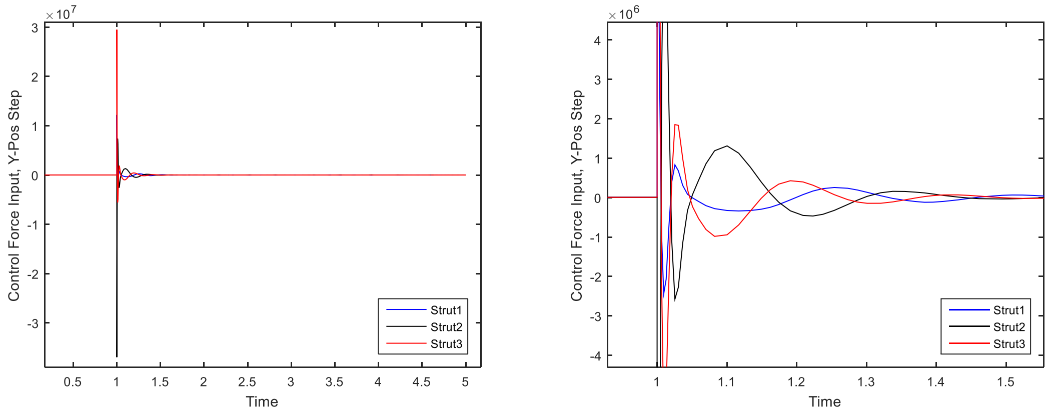

Figure 40: Control Force Input, Y-Pos Step

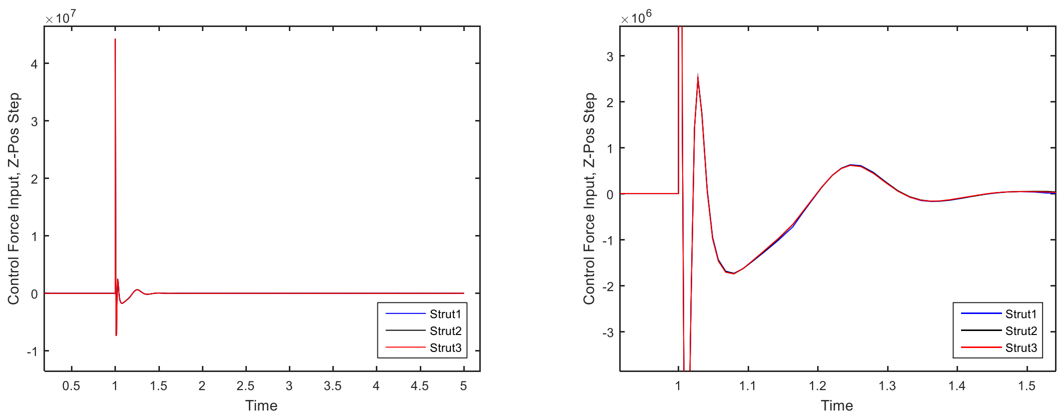

Figure 41: Control Force Input, Z-Pos Step

Figure 42 shows that for initial configuration, the three struts have identical control forces input. This is a good representation of reality, as under initial configuration the only exterior force is gravitational which is along Z-axis, all the tensile force of the string members are symmetrically identical along Z-axis, so they are cancelled out.

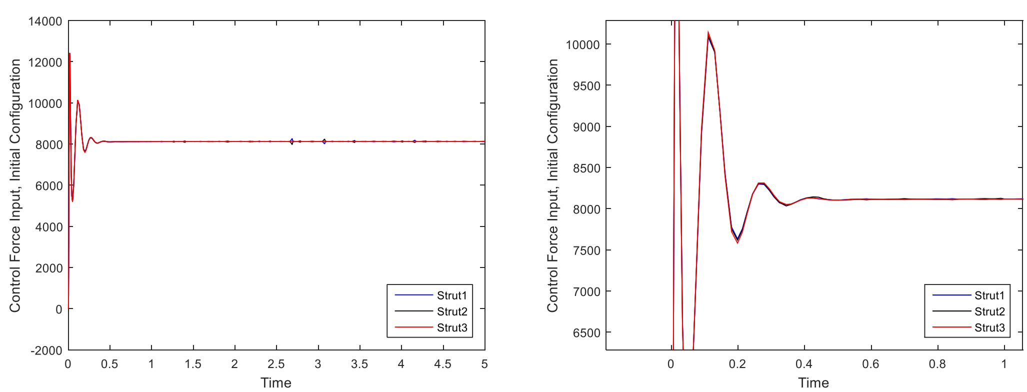

Figure 42: Control Force Input, Initial Configuration.

In step input simulation, for step input in either X-axis and Y-axis, as shown in Figure 36-37, Y positions moved to 0.8, a 0.8 increase from its initial position at 0, Z positions settled at 10.57, a 0.02 decrease from its initial position at 10.59. The difference between the X and Y step responses come to how X position differs, as shown in the plots, they are identical in absolute values with opposite signs.

In Z-axis step input, both X-axis and Y-axis position stayed at their original position at (0,0). Some trivial vibration occurred along X-axis could be a result of PID controller tuning. Z position settled at 11.34 a 0.75 increase from its initial position at 10.59.

We look at the control force input for step response, for step input in either X-axis and Y-axis, as shown in Figure 39-40, strut 3 has identical control force input while strut 1 and strut 2 switches in value, this is also a true representation in real-world as X and Y axis are orthogonal and strut 1 and 2 are positioned in symmetric with each other in terms of X and Y axes.

In Z-axis step input, control forces of all three struts move in an identically synchronized manner to lift the structure to its new position which is at $(0,0,11.34)$, Z position settled at 11.34 a 0.75 increase from its initial position at 10.59.

It can also be observed that for the step-input response, structure settles in a relevant fast manner, around 1 second from receiving the input to completely damps out vibrations., however, there was an overshoot of approximately 50%- 60% of the specified step command. Keep in mind that for the step response, PID controllers were not retuned to achieve our desired performance, as it was not within the scope of this thesis.

CHAPTER 5: CONCLUSIONS

In this thesis, we provided a literature overview of the current tensegrity research field to lay the background for our study. We also reviewed major form-finding methods to build the tensegrity structure for our simulation. Next, structure analysis using Lagrangian methods has been carried out for a 3-strut tensegrity table application. Equations of motions were obtained from calculation.

As the main goal of this thesis, we have employed SimMechanics software to model tensegrity structure, for both static and dynamic simulation purposes. Detailed modeling procedure has been provided on how to build a class-2 5-layer and 3-layer tensegrity tower. To represent physical models more accurately, our research contributed in two major areas: 1) the construction of tensile members (strings) in SimMechanics, 2) modeling of shaker table with chirp signal input for forced vibration experiments. A transient response study was performed to determine the correlation between the string parameter and system vibration characteristics. The results conform to experimental and analytical conclusions. We also did forced vibration and bending mode simulation, and compared findings to similar studies in the field and were satisfied with our model performance.

To take advantage of the SimMechanics models, a 3-strut tensegrity robot was built with strut actuators and sensors for dynamic control simulation. Two major contributions were made during the process: 1) PID controller for each strut has been integrated into our tensegrity structure, 2) leg trajectory block was developed to allow individual input to X, Y and Z positions. Another transient response study was done to verify the model performance and results were consistent with results from the first model. PID control algorithm was fine-tuned independently to improve model response. Next, the step-input response was studied and the correlation between X, Y and Z controller inputs and position of top plates. The results were according to analytical results. The control forces were high due to structure and controllers were not optimized for the specific structure maneuver. In order to achieve desired control objective with smaller control force input, a global optimization approach is recommended where the controller attempts to realize the overall minimal value of a function on a given set of conditions.

Our research indicates that the SimMechanics modeling and simulation approach provides an accurate representation to real-world tensegrity structures. Static and dynamic simulation results conform to findings from physical experiments as well as the analytical process. As tensegrity structures are scalable, shape controllable and also lightweight, this makes them ideal candidates for space applications. Once a single cell has been created, it can be duplicated to multiple cells and together they could form a larger-scale structure. SimMechanics can also be used to aid the design and optimization of tensegrity structures and corresponding controllers. Rapid prototyping and rapid redesign can also be achieved with the help of SimMechanics.

We mentioned in section 4.3.4 that vibration control results could be improved for step input responses. The reason being the PID control algorithm was not optimized for step response. We propose two approaches to address this issue: 1. The automatic retuning of the PID controller can be implemented into each model and needs to be re-run for different application scenarios to achieve control objectives. This can be achieved with modern programming and automation while it could be computationally costly, and the structure can also have low structure control efficiency. 2. A better approach would be, instead of a bottom-up design like the traditional form-finding method, we employ a top-down design approach, to understand the user demand and control mission and then come up with a tensegrity structure that fits that objective. That way, we can design the structure within the optimal controller operating envelope, thus achieve better overall control efficiency.

CHAPTER 6: FUTURE WORK

The PID controller we developed provided acceptable control results for initial control simulation with step responses input. In more complex applications such as tensegrity based flight simulator, it has 6 degree-of-freedom and would require multiple simultaneous control inputs to maneuver the structures. Aside from the before-mentioned design approach. It would be necessary to study advanced control algorithms such as robust control and fuzzy logic control. Artificial intelligence approaches such as artificial neural network and evolutionary algorithms can also be implemented into the analysis and design of structure and controllers. Once a controller has been modeled in the Simulink environment, it can be easily integrated into the SimMechanics tensegrity models.

In space application, there has been a demand for lightweight structures that can be stored in a compact form and quickly deployable into shapes when in position. Think of an example in transferring of liquid propellants between spacecraft aka space refuelling, the research has been traditionally challenging due to the microgravity environment. Shown in Figure 43, the tensegrity structure with fuel line inside provides a flexible yet rigid connection between the tanker and receiver, the tensegrity structure will also have maneuverable capabilities as shown in our research which can assist the initial docking process. Progress made in this research field is critical in weight saving and cost reduction for space missions.

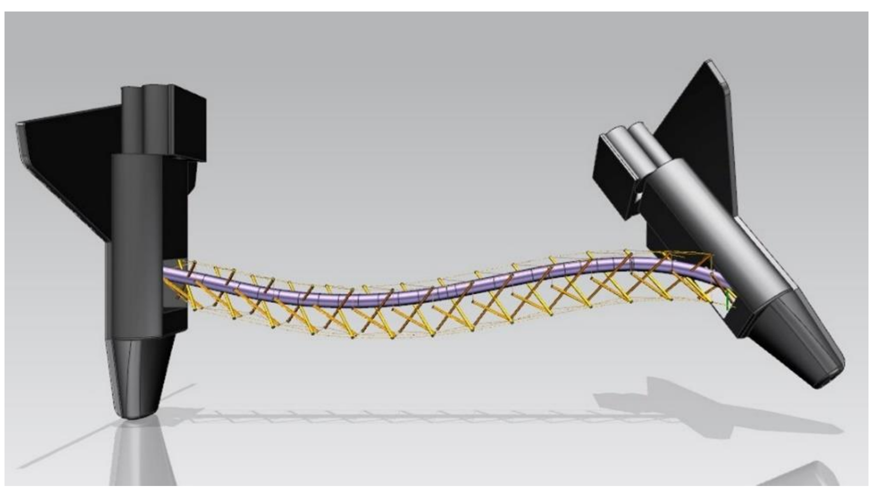

Figure 43: Tensegrity Refuelling Solution for Spacecrafts

In military application, it is critical to provide access routes and to restore vital lifelines for troops during military operations. In that case, a portable tensegrity bridge can be developed that is lightweight to be carried by troops yet strong enough to sustain the weight of hundreds to thousands of pounds, as shown in Figure 44. Another example is a deployable military tent that can provide shelter for hundreds of people or as combat hospitals, and also compact enough to be carried by regular pickup trucks, as shown in Figure 45.

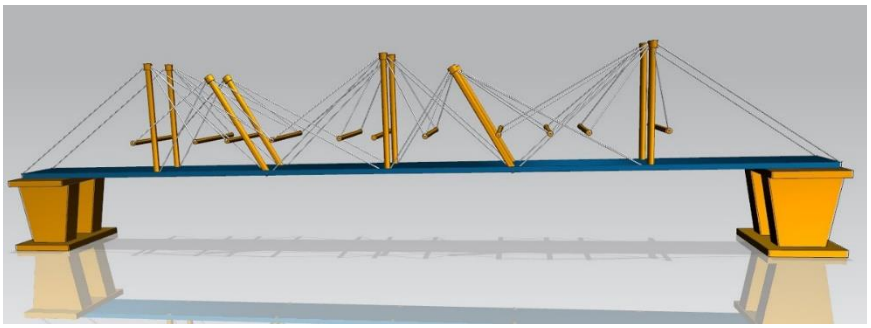

Figure 44: Tensegrity Field-Deployable Bridge

Figure 45: Tensegrity Truck-Deployable Tent

We are in the age of development in interstellar travel and modern warfare; there is a growing need for smart structures and research resources are pouring in both from NASA, DoD and the private sectors such as SpaceX. Our study using SimMechanics modeling approach has proven to have great potential to provide an effective and accurate research tool in the tensegrity modeling and simulation field.

REFERENCES

[1] R. Skelton, Tensegrity Systems, United Sates: Springer-Verlag, 2009.

[2] "The X-module," [Online]. Available: http://www.tensegriteit.nl/e-xmodule.html. [Accessed 10 1 2020].

[3] R. Skelton, R. Adhikari, J. Pinaud, W. Chan and J. Helton, "An Introduction to the Mechanics of Tensegrity Structures," in *Proceedings of the 40th IEEE Conference on Decision and Control*, 2001.

[4] K. Snelson, "The Art of Tensegrity," *International Journal of Space Structures,* vol. 27, no. 2-3, pp. 71-80, Jun.2012.

[5] "TENSEGRITY," [Online]. Available: http://www.tensegriteit.nl/e-simple.html. [Accessed 1 10 2020].

[6] Y. D. Bansod, D. Nandanwar and J. Bursa, "Overview of tensegrity—I: basic structures," *Engineering Mechanics,* vol. 21, pp. 355-367, 2014.

[7] R. B. Fuller, Synergetics: explorations in the geometry of thinking, Macmillan, 1982.

[8] K. D. Snelson, "Snelson on The Tensegrity Invention," *International Journal of Space Structures,* vol. 11, pp. 43-48, 1996.

[9] C. Sultan, M. Corless and R. E. Skelton, "The prestressability problem of tensegrity structures. Some analytic solutions," *International Journal of Solids Structures,* vol. 38 (1), pp. 5223-5252, 2001.

[10] H. Kenner, Geodesic Math and How to Use It, Berkeley: University of California Press, 1976.

[11] A. Hanaor and R. Levy, "Evaluation of deployable structures for space enclosures," *International*

Journal of Space Structures, vol. 16(4), pp. 211-229, 2001.

[12] V. G. Jauregui, "Tensegrity structures and their application to architecture," MS. Thesis, Queen's University, UK, 2010.

[13] J. N. Maina, "Spectacularly robust! Tensegrity principle explains the mechanical strength of the avian lung," *Respiratory Physiology & Neurobiology,* vol. 155, no. 1, pp. 1-10, 2007.

[14] Y. Li, X. Q. Feng, Y. Q. Cao and H. Gao, "A Monte Carlo form-finding method for large scale regular and irregular tensegrity structures," *International Journal of Solids and Structures,* vol. 47, no. 14-15, pp. 1888-1898, 2010.

[15] H. J. Schek, "The force density method for form finding and computation of general networks," *Computer Methods in Applied Mechanics and Engineering,* vol. 3, no. 1, pp. 115-134, 1974.

[16] I. Stern, "Deployable reflector antenna with tensegrity support architecture and associated methods". US Patent Patent No. US 6542132 B2, 2003.

[17] A. G. Tibert and S. Pellegrino, "Review of form-finding methods for tensegrity structures," *International Journal of Space Structures,* vol. 26, no. 3, pp. 241-255, 2011.

[18] L. Zhang, H. Zhao and X. Feng, "Constructing large-scale tensegrity structures with bar–bar connection using prismatic elementary cells," *Applied Mechanics,* vol. 85, no. 3, pp. 383-394, 2015.

[19] R. Motro, "Tensegrity systems: the state of the art," *International Journal of Space Structures,* vol. 7, no. 2, pp. 75-83, 1992.

[20] N. Ali and I. Smith, "Dynamic behavior and vibration control of a tensegrity structure," *International Journal of Solids and Structures,* vol. 47, no. 9, pp. 1285-1296, 2010.

[21] C. Sultan and R. E. Skelton, "Tendon control deployment of tensegrity Structures," in *Proceeding of SPIE, 5th International Symposium on Smart Structures and Material*, San Diego, 1998.

[22] P. Glenn and C. Kelly, "Dynamic Modeling of Morphing Tensegrity Structures," in *AIAA Infotech at Aerospace Conference and Exhibit*, 2011.

[23] V. Vassart and R. Motro, "Tensegrity systems," *International Journal of Space Structures,* vol. 18, no. 2, pp. 77-84, 2003.

[24] R. Connelly and A. Back, "Mathematics and Tensegrity," *American Scientist,* vol. 86, no. 2, pp. 142-151, 1998.

[25] H. C. Tran and J. Lee, "Advanced form-finding of tensegrity structures," *Computers & Structures,* vol. 88, no. 3, pp. 237-246, 2010.

[26] M. R. Barnes, "Form finding and analysis of tension structures by dynamic relaxation," *International Journal of Space Structures,* vol. 14, no. 2, pp. 89-104, 1999.

[27] B. Domer, E. Fest, V. Lalit and I. Smith, "Combining dynamic relaxation method with artificial neural networks to enhance simulation of tensegrity structures," *Journal of Structural Engineering,* vol. 129, no. 5, pp. 672-681, 2003.

[28] The MathWorks, Inc., SimMechanics Users Guide, Natick, 2006.

[29] T. Denery, J. R. Ghidella, P. J. Mosterman and R. Shenoy, "Creating Flight Simulator Landing Gear Models Using Multidomain Modeling Tools," in *AIAA Modeling and Simulation Technologies Conference and Exhibit*, Colorado, 2006.

[30] D. W. Giles, Simulating mechanical systems in simulink with SimMechanics, Natick: The MathWorks, Inc., 2003.

[31] W. L. Chan, D. Arbelaez, F. Bossens and R. E. Skelton , "Active vibration control of a three-stage tensegrity structure," in *SPIE 11th Annual International Symposium on Smart Structures and Materials*, 2004.

[32] R. Cross, C. Lindsey and D. Andruczyk, "Laboratory testing of tennis strings," *Sports Engineering,* vol. 3, no. 4, pp. 219-230, 2001.

[33] M. Pollakowski and H. Ermer, "Chirp Signal Matching and Signal Power Optimization in Pulse-Echo Mode Ultrasonic Nondestructive Testing," *Ultrasonics, Ferroelectrics and Frequency Control,* vol. 41, no. 5, pp. 655-659, 1994.

[34] P. M. Djuric and S. M. Kay, "Parameter estimation of chirp signals," *IEEE Transactions on Acoustics, Speech, and Signal Processing,* vol. 38, pp. 2118-2126, 1990.

[35] F. Wang and C. K. Mechefske, "Adaptive modeling of transient vibration signals," *Mechanical System Signal Process,* vol. 20, pp. 825-842, 2006.

[36] M. Jones and K. Cohen, "Fuzzy Control of a Tensegrity Based Morphing UAV Wing," in *AIAA Infotech at Aerospace Conference and Exhibit*, 2011.